

Rapid Boundary Stabilization of Two-Dimensional Elastic Plates with In-Domain Aeroelastic Instabilities

Xingzhi Huang ^a and Ji Wang ^a

^a*School of Aerospace Engineering, Xiamen University, Xiamen*

Abstract

Motivated by active wing flutter suppression in high-Mach-number flight, this paper presents a rapid boundary stabilization strategy for a two-dimensional PDE-modeled elastic plate with in-domain instabilities, where the exponential stability is achieved with a decay rate that can be arbitrarily assigned by the users. First, the aeroelastic system is modeled as two-dimensional coupled wave PDEs with internal anti-damping terms, derived by Piston theory and Hamilton's principle. Using Fourier series expansion, the 2-D problem is decomposed into a parameterized family of 1-D systems. For each mode, a full-state boundary feedback controller is designed via PDE backstepping transformation. To enable output-feedback implementation, a state observer is further designed to estimate the distributed states over the two-dimensional spatial domain. Through Lyapunov analysis, the exponential stability of the 2-D elastic plate PDE under the proposed boundary control is established with a designer-tunable decay rate. Numerical simulations verify the effectiveness of the control strategy in suppressing flow-induced vibrations.

Key words: Boundary control; Two-dimensional hyperbolic PDEs; Backstepping; Aeroelastic flutter suppression.

1 Introduction

1.1 Motivation

Modern flying-wing aircraft are characterized by low mass and low wing bending natural frequencies. In high-Mach-number flight regimes, unsteady aerodynamic loads strongly interact with the elastic wing dynamics, resulting in aeroelastic flutter. This instability severely constrains the flight envelope and degrades the mission capability of the aircraft. The underlying physics of the flexible wing under aerodynamic loading can be accurately captured by a two-dimensional elastic plate model featuring spatially destabilizing flow-induced terms. From this perspective, active wing flutter suppression can be naturally formulated as a boundary control problem for a two-dimensional elastic plate, which can be modeled as a group of two-dimensional coupled wave PDEs, with in-domain instabilities.

1.2 Boundary control of two-dimensional elastic plates

Early work by Lagnese in 1989 proposed boundary actuation to stabilize elastic plates [17]. Subsequently, Rao demonstrated that boundary control can effectively suppress transverse vibrations of elastic plates under certain boundary conditions [18]. Using Rao's approach, Liu et al. [19] arrived at the same conclusions as Lagnese, but they only achieved asymptotic stability rather than exponential stability. Recent research by Bouhamed et al. [4] presents the problem of optimal control of a nonlinear Kirchhoff plate equation by a bilinear control on the boundary. However, most existing results focus on systems with inherent internal damping and therefore do not address the more challenging case of plates with in-domain instabilities. Boundary control of flexible or compliant structures exhibiting instabilities has been studied using the backstepping method. However, the available results are largely restricted to one-dimensional structures, such as compliant cables and flexible beams, as shown in Table 1. Boundary control designs for 2-D plate structures with in-domain instability are rare.

1.3 Higher-dimensional backstepping control of PDEs

In recent decades, significant progress has been made in PDE control. Among various established methodologies,

* This paper was not presented at any IFAC meeting.

Email addresses: 34520241151610@stu.xmu.edu.cn (Xingzhi Huang), jiwang9024@gmail.com (Ji Wang).

Table 1
Backstepping boundary control for compliant or flexible structures.

Category	References
Compliant Cables/Strings	[1],[5],[6],[35],[36],[37]
Flexible Beams	[7],[15],[16],[24],[34]
Flexible Plates	This paper

the backstepping approach has demonstrated notable effectiveness, offering a systematic framework for boundary feedback design, primarily for one-dimensional parabolic and hyperbolic systems. Extending backstepping to higher spatial dimensions presents considerable challenges, largely due to the increased complexity of the resulting kernel equations. Advances in this direction have been achieved by utilizing specific geometric symmetries and boundary conditions to simplify these equations. Initial breakthroughs in multidimensional control, particularly in fluid flow applications, made use of spatial invariance [3]. This approach transformed the original system into families of parameterized one-dimensional PDEs via Fourier transforms [26], a technique later employed in the control of convection loops [27] and magnetohydrodynamic flows [39]. For domains exhibiting radial symmetry, such as disks [29], spheres [31], and n-dimensional balls [30], explicit backstepping controllers have been derived using spherical harmonics and Bessel functions. More recent developments address systems with spatially varying coefficients on arbitrary-dimensional balls [28] and extend the methodology to three-dimensional multi-agent systems [23,41,38], as well as to PDEs coupled with lower-dimensional boundary dynamics [33]. Besides, [10,11] developed a bilateral delay-compensation control strategy for an unstable 2-D reaction-diffusion system with distinct input delays.

Despite these advances, existing theoretical results are largely confined to parabolic PDEs. In contrast, the active suppression of wing flutter in high-Mach-number flight regimes calls for boundary control frameworks of high-dimensional coupled wave PDEs with in-domain unstable sources, which remain largely unexplored.

1.4 Main Contribution

- 1) The work [7] addressed state-feedback boundary control of one-dimensional beam systems by rewriting it into a class of coupled hyperbolic PDEs [8,13,21,32,14]. Here, we address output-feedback boundary control of two-dimensional plate models, accounting for more complex couplings among three-directional vibrations.
- 2) Different from the boundary control of high-dimensional PDEs investigated in [23,41,38,26,28,33,10,11] for parabolic PDEs, this work deals with a group of coupled wave PDEs with instability sources in two dimensions.

3) To the best of our knowledge, this is the first result of rapid boundary stabilizing a two-dimensional elastic plate with anti-stable sources in the spatial domain, where the decay rate can be arbitrarily assigned by users.

1.5 Notation

- The notation $|\cdot|$ denotes Euclidean norm. The notation $\dot{z}(t)$ denotes the time derivative of z . The notation $c^{(i)}(x)$ denote the i times derivatives of c .
- Let $\Omega \subset \mathbb{R}^n$ be an open set, and let $x = (x_1, \dots, x_n) \in \Omega$ denote the spatial variable. The space $L^2(\Omega)$ consists of all measurable functions $f : \Omega \rightarrow \mathbb{R}$ such that $\int_{\Omega} |f(x)|^2 dx < \infty$, with norm $\|f\|_{L^2(\Omega)} = (\int_{\Omega} |f(x)|^2 dx)^{1/2}$. The Sobolev space $H^1(\Omega)$ is defined as $H^1(\Omega) = \{f \in L^2(\Omega) : \partial_{x_i} f \in L^2(\Omega), i = 1, \dots, n\}$, where $\partial_{x_i} f$ denotes the weak partial derivative with respect to x_i . The norm in $H^1(\Omega)$ is given by $\|f\|_{H^1(\Omega)} = \left(\|f\|_{L^2(\Omega)}^2 + \sum_{i=1}^n \|\partial_{x_i} f\|_{L^2(\Omega)}^2 \right)^{1/2}$.

2 Modeling

2.1 Modeling of aerodynamic forces

We consider an aeroelastic system shown in Fig.1, with the band $0 < x^* < L_1^*, 0 < y^* < L_2^*, z^* = 0$, where L_1^* and L_2^* are the length of the plate in x^* , y^* direction, respectively, representing a two-dimensional elastic plate with flow in the x^* direction.

The physical models used in treating fluid-structure interaction phenomena vary enormously in their complexity and range of applicability. The simplest model is the very popular "Piston theory". Based on Piston theory [9], the local aerodynamic pressure exerted by local fluid velocity normal to the elastic plate is given by

$$p^*(t^*, x^*, y^*) = \frac{\rho_f^* U^*}{M^*} (w_{t^*}^* + U^* w_{x^*}^*), \quad (1)$$

where $w^*(t^*, x^*, y^*)$ is the displacement of the plate in z^* direction at the axial location (x^*, y^*) at time t^* , and ρ_f^* , U^* and M^* are the free stream density, velocity, and Mach number [9], respectively.

2.2 Equations of motion and boundary conditions via Hamilton's Principle

The modeling process follows the approach in [12]. The equation of motion is obtained using Hamilton's variation principle. According to Kirchhoff Plate Theory in [22] and ignore the influence of Poisson's ratio, the potential energy due to bending is given by

$$PE_{bending}^* = \frac{D^*}{2} \int_0^{L_1^*} \int_0^{L_2^*} [(w_{x^* x^*}^*)^2 + (w_{y^* y^*}^*)^2 + (w_{x^* y^*}^* + w_{y^* x^*}^*)^2] dx^* dy^*, \quad (2)$$

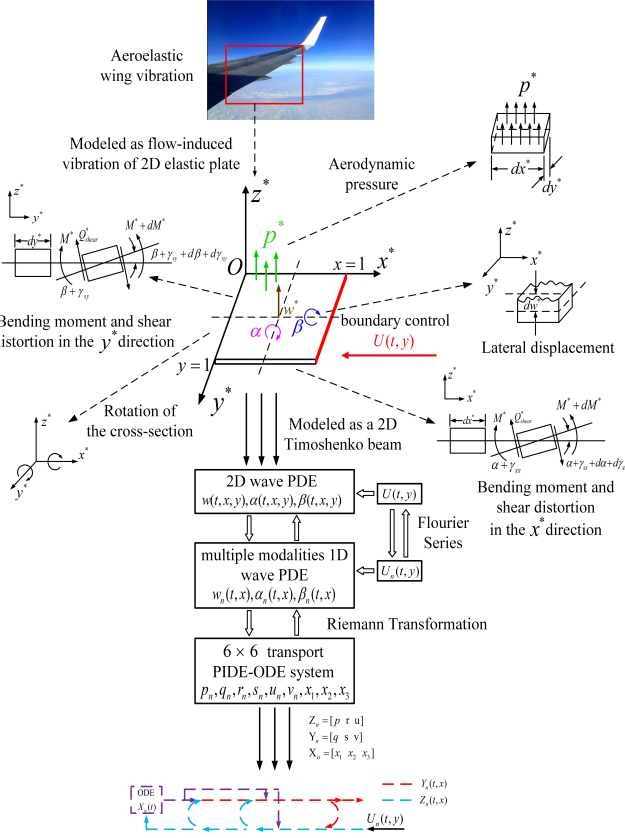


Fig. 1. Flow-induced vibration wing: from the physical model to the mathematical plant.

where $D^* = \frac{E^* h^*}{12}$ presents the stiffness of a homogeneous plate of orthotropic material which can be defined as $E^* I^*$, where E^* is the modulus of elasticity and $I^* = \frac{h^*}{12}$ is the equivalent cross-sectional moment of inertia about the neutral axis. This model adds the effect of shear distortion (but not rotary inertia). We introduce variables α and β , representing the angle of rotation of the cross-section due to the bending moment in x^* direction and y^* direction respectively, and γ_{sx} , γ_{sy} , the angle of distortion due to shear in x^* and y^* direction. The total angle of rotation in x^* direction is the sum of α and γ_{sx} and the sum of β and γ_{sy} in y^* direction, and is approximately the first derivative of the deflection:

$$\alpha + \gamma_{sx} = w_{x^*}^*, \quad \beta + \gamma_{sy} = w_{y^*}^*. \quad (3)$$

Therefore, the potential energy due to bending given in equation (2) is slightly modified in this case such that

$$PE_{bending}^* = \frac{E^* I^*}{2} \int_0^{L_1^*} \int_0^{L_2^*} [(\alpha_{x^*})^2 + (\beta_{y^*})^2 + (\alpha_{y^*} + \beta_{x^*})^2] dx^* dy^*. \quad (4)$$

The potential energy due to shear is given by

$$PE_{shear}^* = \frac{k' G^* h^*}{2} \int_0^{L_1^*} \int_0^{L_2^*} [(w_{x^*}^* - \alpha)^2 + (w_{y^*}^* - \beta)^2] dx^* dy^*. \quad (5)$$

$$+ (w_{y^*}^* - \beta)^2] dx^* dy^*. \quad (5)$$

where k' is the shape factor, G^* is the shear modulus and h^* is the thickness of the plate. The kinetic energy due to displacement is given by

$$KE_{trans}^* = \frac{\rho^* h^*}{2} \int_0^{L_1^*} \int_0^{L_2^*} (w_{t^*}^*)^2 dx^* dy^*, \quad (6)$$

where ρ^* is the density of the elastic plate. The kinetic energy due to the rotation of the cross-section is given by

$$KE_{rot}^* = \frac{\rho^*}{2} \int_0^{L_1^*} \int_0^{L_2^*} [I_1^* (w_{x^* t^*}^*)^2 + I_2^* (w_{y^* t^*}^*)^2] dx^* dy^*, \quad (7)$$

where I_1^* and I_2^* are the moments of inertia of the plate in the x and y directions, respectively.

In this model we assume that there is no rotational kinetic energy associated with shear distortion, but only with rotation due to bending. Therefore, the kinetic energy term due to rotation is modified to include only the angle of rotation due to bending by replacing $w_{x^*}^*$ with α and $w_{y^*}^*$ with β :

$$KE_{rot}^* = \frac{\rho^*}{2} \int_0^{L_1^*} \int_0^{L_2^*} [I_1^* (\alpha_{t^*})^2 + I_2^* (\beta_{t^*})^2] dx^* dy^*. \quad (8)$$

The Lagrangian, defined by kinetic energy-potential energy, is obtained as follows

$$L_{lagr}^* = KE_{trans}^* + KE_{rot}^* - PE_{bending}^* - PE_{shear}^*. \quad (9)$$

The virtual work due to the non-conservative transverse pressure is given by

$$\delta W_{nc}^* = \int_0^{L_1^*} \int_0^{L_2^*} p^* \delta w^* dx^* dy^*. \quad (10)$$

Introducing the following dimensionless parameters

$$\begin{aligned} x &= \frac{x^*}{L_1^*}, y = \frac{y^*}{L_1^*}, L = \frac{L_2^*}{L_1^*}, h = \frac{h^*}{L_1^*}, t = \frac{t^*}{1}, G = \frac{G^* L_1^{*3}}{E^* I^*}, \\ \rho &= \frac{\rho^* L_1^{*5}}{E^* I^*}, I = \frac{I^*}{L_1^{*3}}, I_1 = \frac{I_1^*}{L_1^{*3}}, I_2 = \frac{I_2^*}{L_1^{*3}}, \\ \rho_f &= \frac{\rho_f^* L_1^{*5}}{E^* I^*}, U = \frac{U^*}{L_1^*}, M = \frac{M^*}{1}, p = \frac{p^* L_1^{*3}}{E^* I^*} \end{aligned} \quad (11)$$

In terms of these dimensionless length scales, the dimensionless L_{lagr} defined by $\frac{L_{lagr}^*}{E^* I^*}$ is given by

$$L_{lagr} = \frac{1}{2} \int_0^1 \int_0^L [\rho h w_t^2 + \rho I_1 \alpha_t^2 + \rho I_2 \beta_t^2 - \alpha_x^2 - \beta_y^2 - (\alpha_y + \beta_x)^2 - k' G h (w_x - \alpha + w_y - \beta)^2] dx dy, \quad (12)$$

the dimensionless non-conservative work W_{nc} defined by $\frac{W_{nc}^*}{E^* I^*}$ is given by

$$\delta W_{nc} = \int_0^1 \int_0^L \frac{\rho_f U}{M} (w_t + U w_x) \delta w dx dy. \quad (13)$$

Using the extended Hamilton's principle, by including the non-conservative forcing, the governing differential equation of motion is given by

$$\epsilon w_{tt} = w_{xx} - \alpha_x + w_{yy} - \beta_y + \theta w_t + \xi w_x, \quad (14)$$

$$\mu_1 \alpha_{tt} = \alpha_{xx} + \frac{a}{\epsilon} (w_x - \alpha) + \alpha_{yy} + \beta_{xy}, \quad (15)$$

$$\mu_2 \beta_{tt} = \beta_{yy} + \frac{a}{\epsilon} (w_y - \beta) + \beta_{xx} + \alpha_{yx}, \quad (16)$$

with the following boundary conditions

$$w_x(t, 0, y) = \alpha(t, 0, y), \quad w_y(t, x, L) = \beta(t, x, L), \quad (17)$$

$$\alpha_x(t, 0, y) = 0, \quad \alpha_y(t, x, L) = -\beta_x(t, x, L), \quad (18)$$

$$\beta_x(t, 0, y) = -\alpha_y(t, 0, y), \quad \beta_y(t, x, L) = 0, \quad (19)$$

$$w(t, x, 0) = 0, \quad \alpha(t, x, 0) = 0, \quad \beta_y(t, x, 0) = 0, \quad (20)$$

$$w_x(t, 1, y) = \alpha(t, 1, y) + \frac{1}{k'Gh} U_1(t, y), \quad (21)$$

$$\alpha_x(t, 1, y) = U_2(t, y), \quad (22)$$

$$\beta_x(t, 1, y) = -\alpha_y(t, 1, y) + U_3(t, y), \quad (23)$$

where $\epsilon = \frac{\rho h}{k'Gh}$, $\mu_1 = \rho I_1$, $\mu_2 = \rho I_2$, $a = \rho h$, $\theta = \frac{\rho_f U}{Mk'Gh}$ and $\xi = \frac{\rho_f U^2}{Mk'Gh}$, and where $U_1(t, y)$, and $U_2(t, y)$, $U_3(t, y)$ are boundary control force and bending moments, respectively. At the edge $y = 0$, a clamping boundary is considered, and thus the lateral displacement $w(t, x, 0) = 0$ and the rotational displacement about the y -axis $\alpha(t, x, 0) = 0$. Between the supports and the elastic plate, cylindrical rollers aligned along the x -direction are installed. These rollers allow the plate edge to rotate freely about the x -axis via rolling motion, thereby satisfying the zero-moment condition $\beta_y(t, x, 0) = 0$. Next, we conduct the control based on the 2D elastic plate model (14)–(23).

3 Controller Design

3.1 Decompose the 2D problem into infinite many 1D problems through Fourier Series

Specifically, the boundary conditions in y motivate expanding the solution and control inputs in sine and cosine series, respectively:

$$w(t, x, y) = \sum_{n=0}^{\infty} w_n(t, x) \sin(n\pi \frac{y}{L}), \quad (24)$$

$$\alpha(t, x, y) = \sum_{n=0}^{\infty} \alpha_n(t, x) \sin(n\pi \frac{y}{L}), \quad (25)$$

$$\beta(t, x, y) = \sum_{n=0}^{\infty} \beta_n(t, x) \cos(n\pi \frac{y}{L}), \quad (26)$$

$$U_1(t, y) = \sum_{n=0}^{\infty} U_{1,n}(t) \sin(n\pi \frac{y}{L}), \quad (27)$$

$$U_2(t, y) = \sum_{n=0}^{\infty} U_{2,n}(t) \sin(n\pi \frac{y}{L}), \quad (28)$$

$$U_3(t, y) = \sum_{n=0}^{\infty} U_{3,n}(t) \cos(n\pi \frac{y}{L}). \quad (29)$$

This expansion effectively decomposes the 2D problem into countably many 1D problems, each corresponding

to a different sine or cosine mode. For each mode n :

$$\begin{aligned} \epsilon w_{n,tt} &= w_{n,xx} - \alpha_{n,x} - \frac{n^2\pi^2}{L^2} w_n + \frac{n\pi}{L} \beta_n + \theta w_{n,t} \\ &\quad + \xi w_{n,x}, \end{aligned} \quad (30)$$

$$\mu_1 \alpha_{n,tt} = \alpha_{n,xx} + \frac{a}{\epsilon} (w_{n,x} - \alpha_n) - \frac{n^2\pi^2}{L^2} \alpha_n - \frac{n\pi}{L} \beta_{n,x}, \quad (31)$$

$$\mu_2 \beta_{n,tt} = \beta_{n,xx} - \frac{n^2\pi^2}{L^2} \beta_n + \frac{a}{\epsilon} (\frac{n\pi}{L} w_n - \beta_n) + \frac{n\pi}{L} \alpha_{n,x}, \quad (32)$$

with boundary conditions:

$$w_{n,x}(t, 0) = \alpha_n(t, 0), \quad w_{n,x}(t, 1) = U_{4,n}(t), \quad (33)$$

$$\alpha_{n,x}(t, 0) = 0, \quad \alpha_{n,x}(t, 1) = U_{2,n}(t), \quad (34)$$

$$\beta_{n,x}(t, 0) = -\frac{n\pi}{L} \alpha_n(t, 0), \quad \beta_{n,x}(t, 1) = U_{5,n}(t), \quad (35)$$

where $U_{4,n}(t) = U_{1,n}(t)/(k'Gh) + \alpha_n(t, 1)$ and $U_{5,n}(t) = U_{3,n}(t) - \frac{n\pi}{L} \alpha_n(t, 1)$. Therefore, we obtain the 1D Timoshenko beam model represented by the PDE system (30)–(35) for each mode n .

In what follows, we will drop the subscription n for brevity whenever no confusion arises.

3.2 Transformation to coupled transport PIDEs

Following the classical Riemann transformation, the Timoshenko beam for each mode n can be mapped into a first-order hyperbolic integro-differential system coupled with ODEs. Furthermore, in order to remove the diagonal coupling terms, we use a change of coordinates as presented in [40]. The system becomes a 6×6 system of 1D hyperbolic PDEs coupled with three ODEs without diagonal coupling terms by using the following transformation:

$$p = \exp(\sqrt{\epsilon} \bar{c}_1 x) (w_x + \sqrt{\epsilon} w_t), \quad (36)$$

$$q = \exp(\sqrt{\epsilon} \bar{c}_2 x) (w_x - \sqrt{\epsilon} w_t), \quad (37)$$

$$r = \alpha_x + \sqrt{\mu_1} \alpha_t, \quad s = \alpha_x - \sqrt{\mu_1} \alpha_t, \quad (38)$$

$$u = \beta_x + \sqrt{\mu_2} \beta_t, \quad v = \beta_x - \sqrt{\mu_2} \beta_t, \quad (39)$$

$$x_1 = w(t, 0), \quad x_2 = \alpha(t, 0), \quad x_3 = \beta(t, 0). \quad (40)$$

where $\bar{c}_1 = \frac{\xi}{2\sqrt{\epsilon}} + \frac{\theta}{2\epsilon}$, $\bar{c}_2 = \frac{\xi}{2\sqrt{\epsilon}} - \frac{\theta}{2\epsilon}$. Define

$$Z = \begin{bmatrix} p & r & u \end{bmatrix}^{\top}, Y = \begin{bmatrix} q & s & v \end{bmatrix}^{\top}, X = \begin{bmatrix} x_1 & x_2 & x_3 \end{bmatrix}^{\top},$$

$$U_{\text{in}} = \begin{bmatrix} \exp(-\sqrt{\epsilon} \bar{c}_1) U_p & U_r & U_u \end{bmatrix}^{\top}, \quad (41)$$

where $U_p(t) = U_4(t) + \sqrt{\epsilon} w_t(t, 1)$, $U_r(t) = U_2(t) + \sqrt{\mu_1} \alpha_t(t, 1)$ and $U_u(t) = U_5(t) + \sqrt{\mu_2} \beta_t(t, 1)$ are redefined control variables for this plant. Then, (30)–(35) is

equivalent to the PDE-ODE system in the matrix form:

$$\begin{aligned} Z_t &= \Sigma Z_x + F_{11}(x)(Z + Y) + F_{12}(x)(Z - Y) \\ &\quad + F_{13}(x)X + \int_0^x F_{14}(x, y)Z(t, y)dy \\ &\quad + \int_0^x F_{15}(x, y)Y(t, y)dy, \end{aligned} \quad (42)$$

$$\begin{aligned} Y_t &= -\Sigma Y_x + F_{21}(x)(Z + Y) + F_{22}(x)(Z - Y) \\ &\quad + F_{23}(x)X + \int_0^x F_{24}(x, y)Z(t, y)dy \\ &\quad + \int_0^x F_{25}(x, y)Y(t, y)dy, \end{aligned} \quad (43)$$

$$\dot{X} = AX + \Sigma Z(t, 0), \quad (44)$$

with boundary conditions

$$Z(t, 1) = U_{\text{in}}, \quad (45)$$

$$Y(t, 0) = CZ(t, 0) + DX, \quad (46)$$

where the definition of Σ , $F_{11}(x)$, $F_{12}(x)$, $F_{13}(x)$, $F_{14}(x, y)$, $F_{15}(x, y)$, $F_{21}(x)$, $F_{22}(x)$, $F_{23}(x)$, $F_{24}(x, y)$, $F_{25}(x, y)$, A , C and D are shown in Appendix-A. The system (42)–(46) contains integral coupling terms and the states of ODEs appearing inside the domain of the PDEs. In what follows, without loss of generality, we assume $\frac{1}{\sqrt{\epsilon}} < \frac{1}{\sqrt{\mu_1}} < \frac{1}{\sqrt{\mu_2}}$, the other cases can be treated analogously by switching the order of the states p , r , u in all subsequent steps.

3.3 Backstepping Transformation and Target System

We introduce the following backstepping transformation:

$$\begin{aligned} \sigma &= Z - \int_0^x K(x, y)Z(t, y)dy - \int_0^x L(x, y)Y(t, y)dy \\ &\quad - \Phi(x)X(t), \end{aligned} \quad (47)$$

$$\psi = Y. \quad (48)$$

The gain kernels are 3×3 matrices, i.e., $K(x, y) = \{k_{ij}(x, y)\}_{1 \leq i, j \leq 3}$, $L(x, y) = \{l_{ij}(x, y)\}_{1 \leq i, j \leq 3}$ and $\Phi(x) = \{\phi_{ij}(x)\}_{1 \leq i, j \leq 3}$, where the kernels $K(x, y)$ and $L(x, y)$ are both defined in the triangle domain $\Gamma : \{(x, y) \in \mathbb{R}^2 | 0 \leq y \leq x \leq 1\}$, and where $\Phi(x)$ is defined in $[0, 1]$. They satisfy following equations:

$$\begin{aligned} \Sigma L_x(x, y) - L_y(x, y)\Sigma &= K(x, y)(F_{11}(y) - F_{12}(y)) \\ &\quad + L(x, y)(F_{21}(y) - F_{22}(y)) - \Omega(x)L(x, y) - F_{15}(x, y) \\ &\quad + \int_y^x [K(x, s)F_{15}(s, y) + L(x, s)F_{25}(s, y)] ds, \end{aligned} \quad (49)$$

$$\begin{aligned} \Sigma K_x(x, y) + K_y(x, y)\Sigma &= K(x, y)(F_{11}(y) + F_{12}(y)) \\ &\quad + L(x, y)(F_{21}(y) + F_{22}(y)) - \Omega(x)K(x, y) - F_{14}(x, y) \\ &\quad + \int_y^x [K(x, s)F_{14}(s, y) + L(x, s)F_{24}(s, y)] ds, \end{aligned} \quad (50)$$

$$\begin{aligned} \Phi_x(x) &= \Sigma^{-1}\Phi(x)A - \Sigma^{-1}F_{13}(x) \\ &\quad - \Sigma^{-1}\Omega(x)\Phi(x) + \Sigma^{-1}L(x, 0)\Sigma D \\ &\quad + \int_0^x \Sigma^{-1}(K(x, y)F_{13}(y) + L(x, y)F_{23}(y))dy \end{aligned} \quad (51)$$

with boundary conditions for K and L :

$$\Sigma L(x, x) + L(x, x)\Sigma = -(F_{11}(x) - F_{12}(x)), \quad (52)$$

$$\Sigma K(x, x) - K(x, x)\Sigma = -(F_{11}(x) + F_{12}(x)) + \Omega(x), \quad (53)$$

$$K(x, 0)\Sigma - L(x, 0)\Sigma C = \Phi(x)\Sigma, \quad (54)$$

and with initial conditions for $\Phi(x)$:

$$\Phi(0) = \begin{bmatrix} -\delta_1\sqrt{\epsilon} & 1 & 0 \\ 0 & -\delta_2\sqrt{\mu_1} & 0 \\ 0 & -n\pi & -\delta_3\sqrt{\mu_2} \end{bmatrix} \quad (55)$$

where

$$\Omega(x) = \begin{bmatrix} 0 & \omega_{12} & \omega_{13} \\ 0 & 0 & \omega_{23} \\ 0 & 0 & 0 \end{bmatrix} \quad (56)$$

with $\omega_{12}(x) = (\frac{1}{\sqrt{\epsilon}} - \frac{1}{\sqrt{\mu_1}})k_{12}(x, x) + c_2(x)$, $\omega_{13}(x) = (\frac{1}{\sqrt{\epsilon}} - \frac{1}{\sqrt{\mu_2}})k_{13}(x, x)$, $\omega_{23}(x) = (\frac{1}{\sqrt{\mu_1}} - \frac{1}{\sqrt{\mu_2}})k_{23}(x, x) - \frac{n\pi}{2L\sqrt{\mu_1}}$.

As will be seen in Appendix-E, the parameters δ_1 , δ_2 and δ_3 in (55) are positive design parameters which determine the decay rate of the closed-loop controlled Timoshenko beam.

Applying the above transformation (47), (48), choosing the control law in the boundary (45) as

$$\begin{aligned} U_{\text{in}} &= \int_0^1 K(1, y)Z(t, y)dy + \int_0^1 L(1, y)Y(t, y)dy \\ &\quad + \Phi(1)X(t), \end{aligned} \quad (57)$$

we convert (42)–(46) to the target system:

$$\sigma_t = \Sigma\sigma_x + \Omega(x)\sigma, \quad (58)$$

$$\begin{aligned} \psi_t &= -\Sigma\psi_x + (F_{21}(x) + F_{22}(x))\sigma + (F_{21}(x) - F_{22}(x))\psi \\ &\quad + \int_0^x \Xi_2(x, y)\sigma(t, y)dy + \int_0^x \Xi_3(x, y)\psi(t, y)dy \\ &\quad + \Xi_1(x), \end{aligned} \quad (59)$$

$$\dot{X} = E_1X + \Sigma\sigma(t, 0), \quad (60)$$

with boundary conditions

$$\sigma(t, 1) = 0, \quad \psi(t, 0) = E_2X + C\sigma(t, 0) \quad (61)$$

where

$$E_1 = \Sigma\Phi(0) + A, \quad E_2 = C\Phi(0) + D. \quad (62)$$

The well-posedness of the kernel equations is given in the following theorem.

Theorem 1 There exist unique bounded solutions $k_{ij}(x, y)$, $l_{ij}(x, y)$ and $\phi_{ij}(x, y)$, $i = 1, 2, 3$; $j = 1, 2, 3$ to the kernel equations (49)–(55); in particular, there exists a positive number M such that for $i, j = 1, 2, 3$

$$|k_{ij}(x, y)|, |l_{ij}(x, y)|, |\phi_{ij}(x, y)| \leq M e^{Mx}. \quad (63)$$

Proof. The proof of well-posedness of the kernel equations essentially follows the line in [2], but with the differences that our kernel equations incorporate additional integral terms and ODE to be solved. For the treatment of the ODEs, we draw inspiration from [20]. The complete proof is presented in Appendix-C. \square

Since the kernels in (47) are bounded, the transformation is invertible from the theory of Volterra integral equation, and the inverse backstepping transformation is denoted as:

$$Z = \sigma + \int_0^x \check{K}(x, y)\sigma(t, y)dy + \int_0^x \check{L}(x, y)\psi(t, y)dy + \check{\Phi}(x)X, \quad (64)$$

$$Y = \psi \quad (65)$$

where the kernels $\check{K}(x, y)$, $\check{L}(x, y)$ and $\check{\Phi}(x)$ are also 3×3 matrices, defined in the triangle domain $\Gamma : \{(x, y) \in \mathbb{R}^2 | 0 \leq y \leq x \leq 1\}$, and in $[0, 1]$, respectively. The functions $\Xi_1(x)$, $\Xi_2(x, y)$ and $\Xi_3(x, y)$ in (59) are given by

$$\Xi_1(x) = (F_{21}(x) + F_{22}(x))\check{\Phi}(x) + F_{23}(x) + \int_0^x F_{24}(x, y)\check{\Phi}(y)dy, \quad (66)$$

$$\Xi_2(x, y) = (F_{21}(x) + F_{22}(x))\check{K}(x, y) + F_{24}(x, y) + \int_y^x F_{24}(x, s)\check{K}(s, y)ds, \quad (67)$$

$$\Xi_3(x, y) = (F_{21}(x) + F_{22}(x))\check{L}(x, y) + F_{25}(x, y) + \int_y^x F_{24}(x, s)\check{L}(s, y)ds, \quad (68)$$

where $\Xi_2(x, y)$ and $\Xi_3(x, y)$ are both defined in the triangle domain Γ , and $\Xi_1(x)$ is defined in $[0, 1]$.

3.4 Stabilizing control law and main result

Expressing (57) in terms of the Timoshenko beam variables for each mode n and recalling that $U_{4,n}(t) = \frac{1}{k'Gh}U_{1,n}(t) + \alpha_n(t, 1)$ and $U_{5,n}(t) = U_{3,n}(t) - \frac{n\pi}{L}\alpha_n(t, 1)$, we have

$$\begin{aligned} U_{1,n}(t) &= k'Gh[(\int_0^1 (\mathcal{F}_{11}(\xi)w_n(t, \xi) + \mathcal{F}_{12}(\xi)w_{n,t}(t, \xi) \\ &\quad - \mathcal{F}_{13}(\xi)\alpha_n(t, \xi) + \mathcal{F}_{14}(\xi)\alpha_{n,t}(t, \xi) \\ &\quad - \mathcal{F}_{15}(\xi)\beta_n(t, \xi) + \mathcal{F}_{16}(\xi)\beta_{n,t}(t, \xi))d\xi \\ &\quad + \mathcal{D}_{11}w_n(t, 1) - \mathcal{D}_{12}w_n(t, 0) + \mathcal{D}_{13}\alpha_n(t, 1) \\ &\quad - \mathcal{D}_{14}\alpha_n(t, 0) + \mathcal{D}_{15}\beta_n(t, 1) - \mathcal{D}_{16}\beta_n(t, 0)) \\ &\quad \times \exp(-\sqrt{\epsilon}\bar{c}_1) - \sqrt{\epsilon}w_{n,t}(t, 1) - \alpha_n(t, 1)], \end{aligned} \quad (69)$$

$$\begin{aligned} U_{2,n}(t) &= \int_0^1 (\mathcal{F}_{21}(\xi)w_n(t, \xi) + \mathcal{F}_{22}(\xi)w_{n,t}(t, \xi) \\ &\quad - \mathcal{F}_{23}(\xi)\alpha_n(t, \xi) + \mathcal{F}_{24}(\xi)\alpha_{n,t}(t, \xi) \\ &\quad - \mathcal{F}_{25}(\xi)\beta_n(t, \xi) + \mathcal{F}_{26}(\xi)\beta_{n,t}(t, \xi))d\xi \\ &\quad + \mathcal{D}_{21}w_n(t, 1) - \mathcal{D}_{22}w_n(t, 0) \\ &\quad + \mathcal{D}_{23}\alpha_n(t, 1) - \mathcal{D}_{24}\alpha_n(t, 0) - \sqrt{\mu_1}\alpha_{n,t}(t, 1) \\ &\quad + \mathcal{D}_{25}\beta_n(t, 1) - \mathcal{D}_{26}\beta_n(t, 0), \end{aligned} \quad (70)$$

$$\begin{aligned} U_{3,n}(t) &= \int_0^1 (-\mathcal{F}_{31}(\xi)w_n(t, \xi) + \mathcal{F}_{32}(\xi)w_{n,t}(t, \xi) \\ &\quad - \mathcal{F}_{33}(\xi)\alpha_n(t, \xi) + \mathcal{F}_{34}(\xi)\alpha_{n,t}(t, \xi) \\ &\quad - \mathcal{F}_{35}(\xi)\beta_n(t, \xi) + \mathcal{F}_{36}(\xi)\beta_{n,t}(t, \xi))d\xi \\ &\quad + \mathcal{D}_{31}w_n(t, 1) - \mathcal{D}_{32}w_n(t, 0) \\ &\quad + \mathcal{D}_{33}\alpha_n(t, 1) - \mathcal{D}_{34}\alpha_n(t, 0) \\ &\quad + \mathcal{D}_{35}\beta_n(t, 1) - \mathcal{D}_{36}\beta_n(t, 0) - \sqrt{\mu_2}\beta_{n,t}(t, 1), \end{aligned} \quad (71)$$

where the expressions of $\mathcal{F}ij(\xi)$, \mathcal{D}_{ij} ($i = 1, 2, 3$, $j = 1, 2, 3, 4, 5, 6$) are given in Appendix-B.

The main result for each mode is stated next:

Lemma 1 Consider system (30)–(35) for each mode n , with initial conditions $w_{n,0}, \alpha_{n,0}, \beta_{n,0} \in H^1(0, 1)$, $w_{n,0t}, \alpha_{n,0t}, \beta_{n,0t} \in L^2$, under the control law (69)–(71), for $\delta_1, \delta_2, \delta_3$ satisfying

$$c_n = 2 \min \{\delta_1, \delta_2, \delta_3\} - 1 > 0, \quad (72)$$

then there exists a solution $w_n(t, \cdot)$, $\alpha_n(t, \cdot)$, $\beta_n(t, \cdot) \in H^1(0, 1)$, $w_{n,t}(t, \cdot)$, $\alpha_{n,t}(t, \cdot)$, $\beta_{n,t}(t, \cdot) \in L^2(0, 1)$, and the exponential stability is obtained in the sense of

$$\Omega_n(t) \leq C_n e^{-c_n t} \Omega_n(0), \quad (73)$$

for some positive C_n , where $\Omega_n(t) = \|w_n(t, \cdot)\|_{H^1}^2 + \|\alpha_n(t, \cdot)\|_{H^1}^2 + \|\beta_n(t, \cdot)\|_{H^1}^2 + \|w_{n,t}(t, \cdot)\|_{L^2}^2 + \|\alpha_{n,t}(t, \cdot)\|_{L^2}^2 + \|\beta_{n,t}(t, \cdot)\|_{L^2}^2$.

The proof of Lemma 1 is given in Appendix-E.

Theorem 2 Consider system (14)–(23) under the control law

$$U_1(t, y) = \sum_{n=0}^{\infty} U_{1,n}(t) \sin(n\pi \frac{y}{L}), \quad (74)$$

$$U_2(t, y) = \sum_{n=0}^{\infty} U_{2,n}(t) \sin(n\pi \frac{y}{L}), \quad (75)$$

$$U_3(t, y) = \sum_{n=0}^{\infty} U_{3,n}(t) \cos(n\pi \frac{y}{L}), \quad (76)$$

with initial conditions $w_0, \alpha_0, \beta_0 \in H^1((0, 1)^2)$ and $w_{0,t}, \alpha_{0,t}, \beta_{0,t} \in L^2((0, 1)^2)$. Let $\Omega_a(t)$ denote the total norm

of the 2-D system:

$$\Omega_a(t) = \|w(t, \cdot, \cdot)\|_{H^1}^2 + \|\alpha(t, \cdot, \cdot)\|_{H^1}^2 + \|\beta(t, \cdot, \cdot)\|_{H^1}^2 + \|w_t(t, \cdot, \cdot)\|_{L^2}^2 + \|\alpha_t(t, \cdot, \cdot)\|_{L^2}^2 + \|\beta_t(t, \cdot, \cdot)\|_{L^2}^2, \quad (77)$$

then there exists a constant $D_1 > 0$ and an arbitrary positive number D_2 , which only depends on the arbitrarily positive design parameters δ_1, δ_2 , and δ_3 , such that

$$\Omega_a(t) \leq D_1 e^{-D_2 t} \Omega_a(0). \quad (78)$$

Proof. Recalling the Fourier series (24)–(26), by the Parseval identity, there exist constants $M_n > 0$ such that

$$\Omega_a(t) = \sum_{n=0}^{\infty} M_n \Omega_n(t). \quad (79)$$

Applying (73), we obtain

$$\Omega_a(t) \leq D_1 e^{-D_2 t} \sum_{n=0}^{\infty} M_n \Omega_n(0) \leq D_1 e^{-D_2 t} \Omega_a(0). \quad (80)$$

where $D_1 \geq \max\{C_n\}$, and where $D_2 \leq \min\{c_n\}$, for all n .

We know from Lemma 1 that the constant c_n only depends on the design parameters δ_1, δ_2 and δ_3 . From Appendix-E, we know that the controller design parameters $\delta_1, \delta_2, \delta_3$ are chosen independently of the mode index n . Therefore, D_2 only depends on the arbitrarily positive design parameters δ_1, δ_2 and δ_3 , and it can be set as large as desired by adjusting δ_1, δ_2 and δ_3 . The proof is complete. \square

4 Observer Design

4.1 Observer structure

Next, we present the state observer design for distributed states of the 2-D elastic plates (14)–(23) by using the boundary measurements $w_x(t, 0, y), w_t(t, 0, y), \alpha_x(t, 0, y), \alpha_t(t, 0, y), \beta_x(t, 0, y), \beta_t(t, 0, y), w(t, 0, y), \alpha(t, 0, y)$ and $\beta(t, 0, y)$. This implies that $Z_n(t, 0)$ and $X_n(t)$ are accessible in the equivalent model (42)–(46) via:

$$p_n(t, 0) = 2 \int_0^L (w_x(t, 0, y) + w_t(t, 0, y)) \sin(n\pi \frac{y}{L}) dy, \quad (81)$$

$$r_n(t, 0) = 2 \int_0^L (\alpha_x(t, 0, y) + \alpha_t(t, 0, y)) \sin(n\pi \frac{y}{L}) dy, \quad (82)$$

$$u_n(t, 0) = 2 \int_0^L (\beta_x(t, 0, y) + \beta_t(t, 0, y)) \cos(n\pi \frac{y}{L}) dy, \quad (83)$$

$$x_{1,n}(t) = 2 \int_0^L w(t, 0, y) \sin(n\pi \frac{y}{L}) dy, \quad (84)$$

$$x_{2,n}(t) = 2 \int_0^L \alpha(t, 0, y) \sin(n\pi \frac{y}{L}) dy, \quad (85)$$

$$x_{3,n}(t) = 2 \int_0^L \beta(t, 0, y) \cos(n\pi \frac{y}{L}) dy \quad (86)$$

by estimating (36)–(40) at $x = 0$. In what follows, the state estimates are denoted by a hat, and we drop the subscript n for convenience. Relying on the measurements (81)–(86), recalling that $U_p(t) = U_4(t) + \sqrt{\epsilon} \hat{w}_t(t, 1), U_r(t) = U_2(t) + \sqrt{\mu} \hat{\alpha}_t(t, 1)$ and $U_u(t) = U_5(t) + \sqrt{\mu} \hat{\beta}_t(t, 1)$, and defining

$$\hat{Z} = \begin{bmatrix} \hat{p} & \hat{r} & \hat{u} \end{bmatrix}^T, \hat{Y} = \begin{bmatrix} \hat{q} & \hat{s} & \hat{v} \end{bmatrix}^T, \hat{X} = \begin{bmatrix} \hat{x}_1 & \hat{x}_2 & \hat{x}_3 \end{bmatrix}^T,$$

we build an observer for the equivalent model (42)–(46) as:

$$\begin{aligned} \hat{Z}_t &= \Sigma \hat{Z}_x + F_{11}(x)(\hat{Z} + \hat{Y}) + F_{12}(x)(\hat{Z} - \hat{Y}) \\ &\quad + \int_0^x \left[F_{14}(x, y)\hat{Z}(t, y) + F_{15}(x, y)\hat{Y}(t, y) \right] dy \\ &\quad + P^-(x)(Z(t, 0) - \hat{Z}(t, 0)), \end{aligned} \quad (87)$$

$$\begin{aligned} \hat{Y}_t &= -\Sigma \hat{Y}_x + F_{21}(x)(\hat{Z} + \hat{Y}) + F_{22}(x)(\hat{Z} - \hat{Y}) \\ &\quad + \int_0^x F \left[F_{24}(x, y)\hat{Z}(t, y) + F_{25}(x, y)\hat{Y}(t, y) \right] dy \\ &\quad + P^+(x)(Z(t, 0) - \hat{Z}(t, 0)), \end{aligned} \quad (88)$$

$$\dot{\hat{X}} = AX + \Sigma Z(t, 0) + L_x(X - \hat{X}), \quad (89)$$

with boundary conditions

$$\hat{Z}(t, 1) = U_o(t) + R_1 \hat{Y}(t, 1), \quad (90)$$

$$\hat{Y}(t, 0) = CZ(t, 0) + DX, \quad (91)$$

and where

$$U_o(t) = \begin{bmatrix} h_1 U_4(t) \\ 2U_2(t) \\ 2U_5(t) \end{bmatrix}, R_1 = \begin{bmatrix} h_2 & 0 & 0 \\ 0 & -1 & 0 \\ 0 & 0 & -1 \end{bmatrix}, \quad (92)$$

where $h_1 = \frac{2 \exp(-\sqrt{\epsilon} \bar{c}_1)}{2 - \exp(-\sqrt{\epsilon} \bar{c}_1)}$, $h_2 = \frac{-\exp(-\sqrt{\epsilon} \bar{c}_1)}{2 - \exp(-\sqrt{\epsilon} \bar{c}_1)}$ and $\Sigma, F_{11}(x), F_{12}(x), F_{21}(x), F_{22}(x), F_{14}(x), F_{15}(x), F_{24}(x), F_{25}(x), C$ and D are defined in Appendix-A, and where $P^-(\cdot), P^+(\cdot)$ and L_x are output injection gain matrices yet to be designed.

Recalling the transformation (36)–(40), the estimate of original wave PDEs (30)–(35) are obtained as

$$\begin{cases} \hat{\alpha}_n(t, x) = \left[\int_0^x \frac{\hat{r}_n(t, y) + \hat{s}_n(t, y)}{2} dy + \hat{x}_2(t) \right], \\ \hat{\beta}_n(t, x) = \left[\int_0^x \frac{\hat{u}_n(t, y) + \hat{v}_n(t, y)}{2} dy + \hat{x}_3(t) \right], \\ \hat{w}_n(t, x) = \int_0^x \frac{k_2(y)\hat{p}_n(t, y) + k_1(y)\hat{q}_n(t, y)}{2k_1(y) \cdot k_2(y)} dy + \hat{x}_1(t), \\ \hat{\alpha}_{n,t}(t, x) = \frac{\hat{r}_n(t, x) - \hat{s}_n(t, x)}{2\sqrt{\mu_1}}, \hat{\beta}_{n,t}(t, x) = \frac{\hat{u}_n(t, x) - \hat{v}_n(t, x)}{2\sqrt{\mu_2}}, \\ \hat{w}_{n,t}(t, x) = \frac{k_2(x)\hat{p}_n(t, x) - k_1(x)\hat{q}_n(t, x)}{2\sqrt{\epsilon}(k_1(x) \cdot k_2(x))}, \\ \hat{\alpha}_{n,x}(t, x) = \frac{\hat{r}_n(t, x) + \hat{s}_n(t, x)}{2}, \hat{\beta}_{n,x}(t, x) = \frac{\hat{u}_n(t, x) + \hat{v}_n(t, x)}{2}, \\ \hat{w}_{n,x}(t, x) = \frac{k_2(x)\hat{p}_n(t, x) + k_1(x)\hat{q}_n(t, x)}{2k_1(x) \cdot k_2(x)}, \end{cases} \quad (93)$$

where functions $k_1(x) = \exp(\sqrt{\epsilon}\bar{c}_1 x)$, $k_2(x) = \exp(\sqrt{\epsilon}\bar{c}_2 x)$, and where $\hat{p}_n, \hat{q}_n, \hat{r}_n, \hat{s}_n, \hat{u}_n, \hat{v}_n$ are computed from (87)–(91).

4.2 Observer gains and error systems

Defining the observer errors

$$\tilde{Z} = Z - \hat{Z}, \tilde{Y} = Y - \hat{Y}, \tilde{X} = X - \hat{X}. \quad (94)$$

Subtracting the (87)–(91) from (42)–(46), we get the observer error system:

$$\begin{aligned} \tilde{Z}_t &= \Sigma \tilde{Z}_x + F_{11}(x)(\tilde{Z} + \tilde{Y}) + F_{12}(x)(\tilde{Z} - \tilde{Y}) \\ &\quad + \int_0^x \left[F_{14}(x, y)\tilde{Z}(t, y) + F_{15}(x, y)\tilde{Y}(t, y) \right] dy \\ &\quad - P^-(x)\tilde{Z}(t, 0), \end{aligned} \quad (95)$$

$$\begin{aligned} \tilde{Y}_t &= -\Sigma \tilde{Y}_x + F_{21}(x)(\tilde{Z} + \tilde{Y}) + F_{22}(x)(\tilde{Z} - \tilde{Y}) \\ &\quad + \int_0^x F \left[F_{24}(x, y)\tilde{Z}(t, y) + F_{25}(x, y)\tilde{Y}(t, y) \right] dy \\ &\quad - P^+(x)\tilde{Z}(t, 0), \end{aligned} \quad (96)$$

$$\dot{\tilde{X}} = -L_x \tilde{X}, \quad (97)$$

with boundary conditions

$$\tilde{Z}(t, 1) = R_1 \tilde{Y}(t, 1), \quad \tilde{Y}(t, 0) = 0, \quad (98)$$

where observer gain L_x is

$$L_x = \begin{bmatrix} \frac{L_1}{\sqrt{\epsilon}} & 0 & 0 \\ 0 & \frac{L_2}{\sqrt{\mu_1}} & 0 \\ 0 & 0 & \frac{L_3}{\sqrt{\mu_2}} \end{bmatrix}. \quad (99)$$

The parameters L_1, L_2 , and L_3 are positive design parameters that determine the decay rate of the state \tilde{X} .

To determine the other two observer gains P^- and P^+ , we introduce the following Volterra transformation:

$$\tilde{Z}(t, x) = \tilde{\sigma}(t, x) + \int_0^x N(x, y)\tilde{\sigma}(t, y)dy, \quad (100)$$

$$\tilde{Y}(t, x) = \tilde{\psi}(t, x) + \int_0^x M(x, y)\tilde{\sigma}(t, y)dy, \quad (101)$$

where the kernels N and M defined on $\Gamma = \{(x, y) \in \mathbb{R}^2 | 0 \leq y \leq x \leq 1\}$ satisfy following kernel equations:

$$\begin{aligned} \Sigma M_x(x, y) - M_y(x, y)\Sigma &= (F_{21}(x) - F_{22}(x))M(x, y) \\ &\quad + (F_{21}(x) + F_{22}(x))N(x, y) - M(x, y)\Omega(y) + F_{24}(x, y) \\ &\quad + \int_y^x (F_{24}(x, s)N(s, y) + F_{25}(x, s)M(s, y))ds, \end{aligned} \quad (102)$$

$$\begin{aligned} \Sigma N_x(x, y) + N_y(x, y)\Sigma &= -(F_{11}(x) + F_{12}(x))N(x, y) \\ &\quad - (F_{11}(x) - F_{12}(x))M(x, y) + N(x, y)\Omega(y) - F_{14}(x, y) \\ &\quad - \int_y^x (F_{14}(x, s)N(s, y) + F_{15}(x, s)M(s, y))ds, \end{aligned} \quad (103)$$

with boundary conditions:

$$\Sigma N(x, x) - N(x, x)\Sigma = -(F_{11}(x) + F_{12}(x)) + \Omega(x), \quad (104)$$

$$\Sigma M(x, x) + M(x, x)\Sigma = F_{21}(x) + F_{22}(x), \quad (105)$$

Applying the backstepping transformation (100),(101), and choosing the observer gains P^+, P^- as

$$P^+(x) = M(x, 0)\Sigma, \quad P^-(x) = N(x, 0)\Sigma, \quad (106)$$

we map the observer error system (95)–(98) into the following target system:

$$\begin{aligned} \tilde{\sigma}_t &= \Sigma \tilde{\sigma}_x + (F_{11}(x) - F_{12}(x))\tilde{\psi} + \Omega(x)\tilde{\sigma}(t, x) \\ &\quad + \int_0^x D^-(x, y)\tilde{\psi}(t, y)dy, \end{aligned} \quad (107)$$

$$\begin{aligned} \tilde{\psi}_t &= -\Sigma \tilde{\psi}_x + (F_{21}(x) - F_{22}(x))\tilde{\psi} \\ &\quad + \int_0^x D^+(x, y)\tilde{\psi}(t, y)dy, \end{aligned} \quad (108)$$

$$\dot{\tilde{X}} = -L_x \tilde{X}, \quad (109)$$

with boundary conditions

$$\tilde{\sigma}(t, 1) = R_1 \tilde{\psi}(t, 1), \quad \tilde{\psi}(t, 0) = 0, \quad (110)$$

where

$$\Omega(x) = \begin{bmatrix} 0 & \omega_{12} & \omega_{13} \\ 0 & 0 & \omega_{23} \\ 0 & 0 & 0 \end{bmatrix}, \quad (111)$$

and where D^+, D^- are given by

$$\begin{aligned} D^+(x, y) &= -M(x, y)(F_{11}(y) - F_{12}(y)) \\ &\quad - \int_y^x M(x, s)D^-(s, y)ds + F_{25}(x, y), \end{aligned} \quad (112)$$

$$\begin{aligned} D^-(x, y) &= -N(x, y)(F_{11}(y) - F_{12}(y)) \\ &\quad - \int_y^x N(x, s)D^-(s, y)ds + F_{15}(x, y). \end{aligned} \quad (113)$$

Lemma 2 *There exists a unique bounded solution $m_{ij}(x, y), n_{ij}(x, y)$, $i = 1, 2, 3; j = 1, 2, 3$ to the kernel equations (102)–(105). In particular, there exists some positive number ϕ and D such that for $i, j = 1, 2, 3$*

$$|m_{ij}(x, y)|, |n_{ij}(x, y)| \leq \varphi e^{Dx}. \quad (114)$$

The proof of Lemma 2 is shown in Appendix-D.

4.3 Result of the observer

The following lemma assesses the convergence of the target system to zero.

Lemma 3 Consider system (107)–(109) with initial conditions for $\tilde{X}(0)$ and the output injection kernels given by $P^-(x), P^+(x)$ and L_x , where $P^-(x)$ and $P^+(x)$ are obtained from (106) for each mode n . Choosing the values of the output injection gains L_1, L_2, L_3 to be positive, the observer error system is exponentially stable in the sense of:

$$\begin{cases} \tilde{X}(t) \leq e^{-c'_n t} \tilde{X}(0), t \geq 0 \\ \tilde{\sigma} \equiv \tilde{\psi} \equiv 0, \quad t \geq \frac{2}{\lambda_1}. \end{cases} \quad (115)$$

where $c'_n = \min\{L_1, L_2, L_3\}$, and where $\tilde{\sigma}$ and $\tilde{\psi}$ are bounded in $t \in [0, \frac{2}{\lambda_1}]$.

Proof. Noting (107), (108), we find that the system consists in a cascade of the $\tilde{\psi}$ -system into the $\tilde{\sigma}$ -system. Therefore, by using the method of characteristics, we can easily find that $\tilde{\psi}$ is identically zero for $t \geq \frac{1}{\lambda_1}$. When $t \geq \frac{1}{\lambda_1}$, the $\tilde{\sigma}$ -system becomes:

$$\tilde{\sigma}_t(t, x) - \Sigma \tilde{\sigma}_x(t, x) = \Omega(x) \tilde{\sigma}(t, x), \quad (116)$$

$$\tilde{\sigma}(t, 1) = 0 \quad (117)$$

Noting the particular structure of $\Omega(x)$, the $\tilde{\sigma}$ -system is in fact a cascade of its fast states into its slow states. So one can obtain that $\tilde{\sigma}$ eventually vanishes for

$$t \geq \frac{1}{\lambda_1} + \frac{1}{\lambda_1} = \frac{2}{\lambda_1}. \quad (118)$$

This concludes the proof. \square

Defining

$$\tilde{w} = w - \hat{w}, \tilde{\alpha} = \alpha - \hat{\alpha}, \tilde{\beta} = \beta - \hat{\beta}, \quad (119)$$

the results about the observer error for the original 2-D PDE are given below.

Theorem 3 Considering the observer (87)–(91) together with (93) for each Fourier mode n , constructing the 2D state estimates $\hat{w}(t, x, y) = \sum_{n=0}^{\infty} \hat{w}_n(t, x) \sin(\frac{n\pi y}{L})$, $\hat{\alpha}(t, x, y) = \sum_{n=0}^{\infty} \hat{\alpha}_n(t, x) \sin(\frac{n\pi y}{L})$ and $\hat{\beta}(t, x, y) = \sum_{n=0}^{\infty} \hat{\beta}_n(t, x) \cos(\frac{n\pi y}{L})$, for initial conditions of the resulting observer errors $\tilde{w}_0, \tilde{\alpha}_0, \tilde{\beta}_0 \in H^1((0, 1)^2)$ and $\tilde{w}_{0,t}, \tilde{\alpha}_{0,t}, \tilde{\beta}_{0,t} \in L^2((0, 1)^2)$, the estimates exponentially track the states in the plant (14)–(23) in the sense that there exist a constant $D_3 > 0$ and an arbitrary positive number D_4 such that

$$\Omega_f(t) \leq D_3 e^{-D_4 t} \Omega_f(0). \quad (120)$$

where

$$\begin{aligned} \Omega_f(t) &= \|\tilde{w}(t, \cdot, \cdot)\|_{H^1}^2 + \|\tilde{\alpha}(t, \cdot, \cdot)\|_{H^1}^2 + \|\tilde{\beta}(t, \cdot, \cdot)\|_{H^1}^2 \\ &+ \|\tilde{w}_t(t, \cdot, \cdot)\|_{L^2}^2 + \|\tilde{\alpha}_t(t, \cdot, \cdot)\|_{L^2}^2 + \|\tilde{\beta}_t(t, \cdot, \cdot)\|_{L^2}^2. \end{aligned} \quad (121)$$

Proof. According to Lemma 3, (100), (101), (93), and (E.15), we have

$$\Omega_{nf}(t) \leq H_n e^{-c'_n t} \Omega_{nf}(0), \quad (122)$$

for some positive H_n , where $\Omega_{nf}(t) = \|\tilde{w}_n(t, \cdot)\|_{H^1}^2 + \|\tilde{\alpha}_n(t, \cdot)\|_{H^1}^2 + \|\tilde{\beta}_n(t, \cdot)\|_{H^1}^2 + \|\tilde{w}_{n,t}(t, \cdot)\|_{L^2}^2 + \|\tilde{\alpha}_{n,t}(t, \cdot)\|_{L^2}^2 + \|\tilde{\beta}_{n,t}(t, \cdot)\|_{L^2}^2$. It is obtained from (24)–(26) that $\tilde{w} = \sum_{n=0}^{\infty} \tilde{w}_n(t, x) \sin(n\pi \frac{y}{L})$, $\tilde{\alpha} = \sum_{n=0}^{\infty} \tilde{\alpha}_n(t, x) \sin(n\pi \frac{y}{L})$, $\tilde{\beta} = \sum_{n=0}^{\infty} \tilde{\beta}_n(t, x) \cos(n\pi \frac{y}{L})$, with similar expansions for their time derivatives $\tilde{w}_t, \tilde{\alpha}_t, \tilde{\beta}_t$. Using Parseval's identity, there exist constants $Q_n > 0$ such that

$$\Omega_f(t) = \sum_{n=0}^{\infty} Q_n \Omega_{nf}(t). \quad (123)$$

Applying (122), we obtain

$$\Omega_f(t) \leq D_3 e^{-D_4 t} \sum_{n=0}^{\infty} Q_n \Omega_{nf}(0) \leq D_3 e^{-D_4 t} \Omega_f(0) \quad (124)$$

where $D_3 \geq \max\{H_n\}$ and $D_4 \leq \min\{c'_n\}$, for all n . The proof is complete. We know from Lemma 3 that the constant c'_n only depends on the observer gain parameters L_1, L_2 and L_3 and they can be chosen independently of the mode index n . Therefore, D_4 only depends on the arbitrarily positive design parameters L_1, L_2 and L_3 , and it can be set as large as desired by adjusting L_1, L_2 and L_3 . \square

5 Output-Feedback Control

Combining the full state feedback law with the observer estimates, we obtain a feedback law for each mode n :

$$\begin{aligned} \hat{U}_{1,n}(t) &= k' G h [(\int_0^1 (\mathcal{F}_{11}(\xi) \hat{w}_n(t, \xi) + \mathcal{F}_{12}(\xi) \hat{w}_{n,t}(t, \xi) \\ &- \mathcal{F}_{13}(\xi) \hat{\alpha}_n(t, \xi) + \mathcal{F}_{14}(\xi) \hat{\alpha}_{n,t}(t, \xi)) d\xi \\ &+ \mathcal{D}_{11} \hat{w}_n(t, 1) - \mathcal{D}_{12} w_n(t, 0) + \mathcal{D}_{13} \hat{\alpha}_n(t, 1) \\ &- \mathcal{D}_{14} \alpha_n(t, 0) + \mathcal{D}_{15} \hat{\beta}_n(t, 1) - \mathcal{D}_{16} \beta_n(t, 0)) \\ &\times \exp(-\sqrt{\epsilon} \bar{c}_1) - \sqrt{\epsilon} \hat{w}_{n,t}(t, 1) - \hat{\alpha}_n(t, 1)], \end{aligned} \quad (125)$$

$$\begin{aligned} \hat{U}_{2,n}(t) &= \int_0^1 (\mathcal{F}_{21}(\xi) \hat{w}_n(t, \xi) + \mathcal{F}_{22}(\xi) \hat{w}_{n,t}(t, \xi) \\ &- \mathcal{F}_{23}(\xi) \hat{\alpha}_n(t, \xi) + \mathcal{F}_{24}(\xi) \hat{\alpha}_{n,t}(t, \xi)) d\xi \\ &- \mathcal{F}_{25}(\xi) \hat{\beta}_n(t, \xi) + \mathcal{F}_{26}(\xi) \hat{\beta}_{n,t}(t, \xi) d\xi \\ &+ \mathcal{D}_{21} \hat{w}_n(t, 1) - \mathcal{D}_{22} w_n(t, 0) \\ &+ \mathcal{D}_{23} \hat{\alpha}_n(t, 1) - \mathcal{D}_{24} \alpha_n(t, 0) - \sqrt{\mu_1} \hat{\alpha}_{n,t}(t, 1) \\ &+ \mathcal{D}_{25} \hat{\beta}_n(t, 1) - \mathcal{D}_{26} \beta_n(t, 0), \end{aligned} \quad (126)$$

$$\begin{aligned} \hat{U}_{3,n}(t) &= \int_0^1 (-\mathcal{F}_{31}(\xi) \hat{w}_n(t, \xi) + \mathcal{F}_{32}(\xi) \hat{w}_{n,t}(t, \xi) \\ &- \mathcal{F}_{33}(\xi) \hat{\alpha}_n(t, \xi) + \mathcal{F}_{34}(\xi) \hat{\alpha}_{n,t}(t, \xi)) d\xi \\ &- \mathcal{F}_{35}(\xi) \hat{\beta}_n(t, \xi) + \mathcal{F}_{36}(\xi) \hat{\beta}_{n,t}(t, \xi) d\xi \\ &+ \mathcal{D}_{31} \hat{w}_n(t, 1) - \mathcal{D}_{32} w_n(t, 0) \\ &+ \mathcal{D}_{33} \hat{\alpha}_n(t, 1) - \mathcal{D}_{34} \alpha_n(t, 0) \end{aligned}$$

$$+ \mathcal{D}_{35}\hat{\beta}_n(t, 1) - \mathcal{D}_{36}\beta_n(t, 0) - \sqrt{\mu_2}\hat{\beta}_{n,t}(t, 1), \quad (127)$$

where the values of k_{ij} , l_{ij} and ϕ_{ij} are defined by (49)–(55), and where the estimated states \hat{w}_n , $\hat{\alpha}_n$, $\hat{\beta}_n$, $\hat{w}_{n,t}$, $\hat{\alpha}_{n,t}$ and $\hat{\beta}_{n,t}$ are obtained from (93). Based on (125)–(127) for each mode n , the boundary controller for the original 2-D PDE (14)–(23) is

$$\hat{U}_1(t, y) = \sum_{n=1}^{\infty} \hat{U}_{1,n}(t) \sin(n\pi \frac{y}{L}), \quad (128)$$

$$\hat{U}_2(t, y) = \sum_{n=1}^{\infty} \hat{U}_{2,n}(t) \sin(n\pi \frac{y}{L}), \quad (129)$$

$$\hat{U}_3(t, y) = \sum_{n=0}^{\infty} \hat{U}_{3,n}(t) \cos(n\pi \frac{y}{L}). \quad (130)$$

Theorem 4 Consider the closed-loop system composed of the original plant (14)–(23), the observer (87)–(91), and the control law given by (125)–(130), the exponential stability is achieved in the sense that there exist constants $C_3 > 0$ and $C_4 > 0$ such that

$$\Omega_d(t) \leq C_3 e^{-C_4 t} \Omega_d(0) \quad (131)$$

where C_4 , which only depends on the arbitrarily positive design parameters $\delta_1, \delta_2, \delta_3, L_1, L_2, L_3$, can be arbitrarily assigned by users, and where

$$\begin{aligned} \Omega_d(t) = & \|w(t, \cdot, \cdot)\|_{H^1}^2 + \|\alpha(t, \cdot, \cdot)\|_{H^1}^2 + \|\beta(t, \cdot, \cdot)\|_{H^1}^2 \\ & + \|w_t(t, \cdot, \cdot)\|_{L^2}^2 + \|\alpha_t(t, \cdot, \cdot)\|_{L^2}^2 + \|\beta_t(t, \cdot, \cdot)\|_{L^2}^2 \\ & + \|\hat{w}(t, \cdot, \cdot)\|_{H^1}^2 + \|\hat{\alpha}(t, \cdot, \cdot)\|_{H^1}^2 + \|\hat{\beta}(t, \cdot, \cdot)\|_{H^1}^2 \\ & + \|\hat{w}_t(t, \cdot, \cdot)\|_{L^2}^2 + \|\hat{\alpha}_t(t, \cdot, \cdot)\|_{L^2}^2 + \|\hat{\beta}_t(t, \cdot, \cdot)\|_{L^2}^2. \end{aligned} \quad (132)$$

Proof. Rewriting the output-feedback controller as $\hat{U}_i = U_i + \vartheta_i(t)$, where U_i is the state-feedback control defined in (69)–(71), and where $\vartheta_i(t)$, i.e., the error between the state-feedback and the output-feedback controllers, are exponentially convergent to zero because of Theorem 3. Recalling Theorem 2, and the definition (119), we then obtain (131), where $C_4 \leq \min\{D_2, D_4\}$. The constant D_2 , which only depends on arbitrarily positive design parameters $\delta_1, \delta_2, \delta_3$, is the decay rate given in Theorem 2. The constant D_4 , which only depends on arbitrarily positive design parameters L_1, L_2, L_3 , is the decay rate given in Theorem 3. \square

Remark 1 In practical modeling and control of flexible plates, modal truncation is well justified from an engineering perspective, as high-frequency modes are typically dominated by structural damping and exhibit rapid natural decay. Therefore, as a result, in practical implementation control laws (128)–(130) expressed as infinite modal series can be appropriately approximated by

$$\hat{U}_1(t, y) = \sum_{n=1}^N \hat{U}_{1,n}(t) \sin(n\pi \frac{y}{L}), \quad (133)$$

$$\hat{U}_2(t, y) = \sum_{n=1}^N \hat{U}_{2,n}(t) \sin(n\pi \frac{y}{L}), \quad (134)$$

$$\hat{U}_3(t, y) = \sum_{n=0}^N \hat{U}_{3,n}(t) \cos(n\pi \frac{y}{L}), \quad (135)$$

where N is chosen sufficiently large.

6 Numerical Simulation

The simulation is conducted by finite difference method with a time step of 0.05 and a space step of 0.001. According to Remark 1, we here assume the elastic plate PDE is truncated at $N = 3$ modes under certain operating conditions. The simulation model is (42)–(46), where the plant parameters are $\epsilon = 3$, $\mu_1 = 2$, $\mu_2 = 1$, $a = 0.2$, $\theta = 0.1$, $\xi = 0.2$, $L = 10$, with the modal number $n = 0, 1, 2, 3$. The initial values are set as $x_1(0) = 1$, $x_2(0) = 2$, $x_3(0) = 1$ and $p(0, x) = q(t, 0) = r(t, 0) = s(t, 0) = u(t, 0) = v(t, 0) = 100 \sin(\pi x)$. We apply the proposed output-feedback controller (125)–(127) with the design parameters chosen as $\delta_1 = \delta_2 = \delta_3 = 5$, $L_1 = L_2 = L_3 = 5$, and the gains $K(1, y)$, $L(1, y)$, $\Phi(1)$ are computed using a power series approach as in [25] for corresponding modal number. Using the relationship (E.15) and (93) between the variables $p(t, x)$, $q(t, x)$, $r(t, x)$, $s(t, x)$, $u(t, x)$, $v(t, x)$ and $w(t, x)$, $\alpha(t, x)$, $\beta(t, x)$, we can derive the evolution of $w_n(t, x)$, $\alpha_n(t, x)$, $\beta_n(t, x)$, which, by (24)–(26), are then used to represent the states of the elastic plant $w(t, x, y)$, $\beta(t, x, y)$, $\alpha(t, x, y)$, as shown in the following figures, where the red line highlights the controlled boundary in the 2D domain.

We know from Fig. 2 that the plant is open-loop unstable since the states increase rapidly. Figs. 3–5 show all 2-D states are fast convergent to zero under the proposed boundary control, as expected in Theorem 4. Additionally, Fig. 6–8 shows that the observer errors of these 2-D states, i.e., $\tilde{w}(t, x, y)$, $\tilde{\beta}(t, x, y)$, $\tilde{\alpha}(t, x, y)$ are also convergent to zero, which demonstrates that the proposed observer rapidly converges to the actual PDE states. The observer-based output-feedback boundary control inputs $U_1(t, y)$, $U_2(t, y)$, $U_3(t, y)$ of the 2-D plant (14)–(23) are also calculated by summing the modal components (125)–(127) via (133)–(135), as shown in Fig. 9.

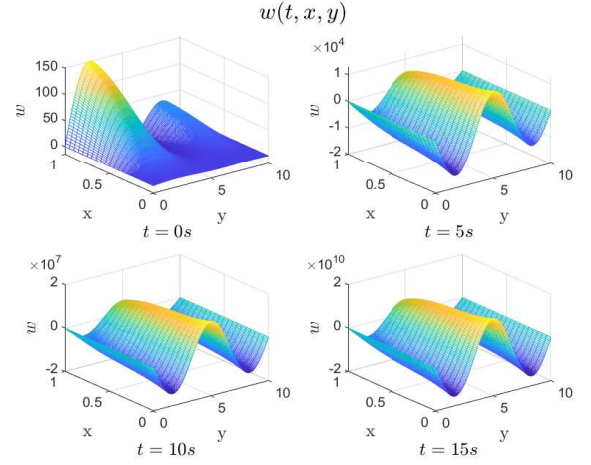


Fig. 2. Results in the open loop.

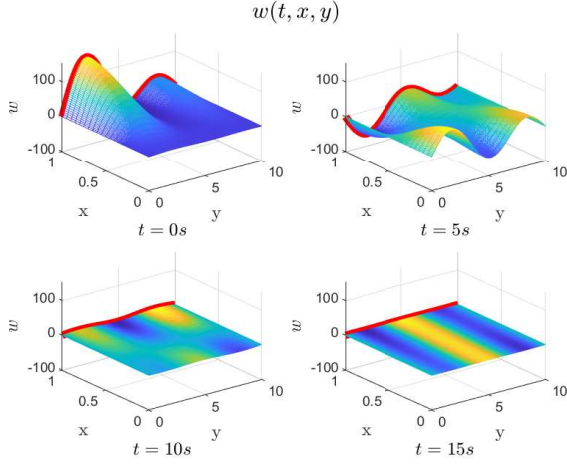


Fig. 3. $w(t, x, y)$ under the proposed observer-based output-feedback boundary controller.

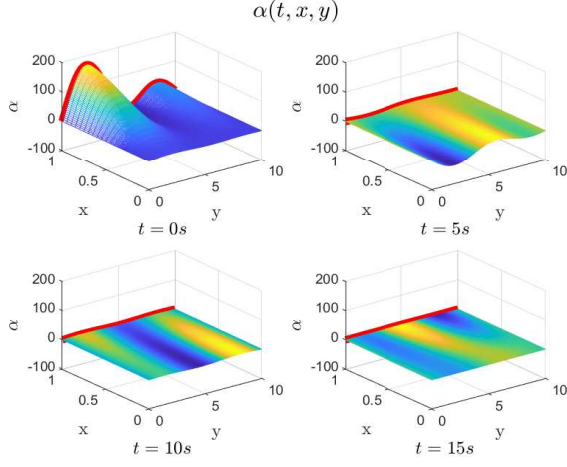


Fig. 4. $\alpha(t, x, y)$ under the proposed observer-based output-feedback boundary controller.

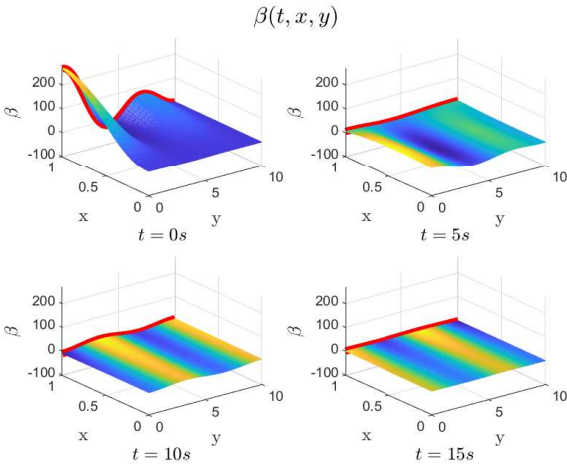


Fig. 5. $\beta(t, x, y)$ under the proposed observer-based output-feedback boundary controller.

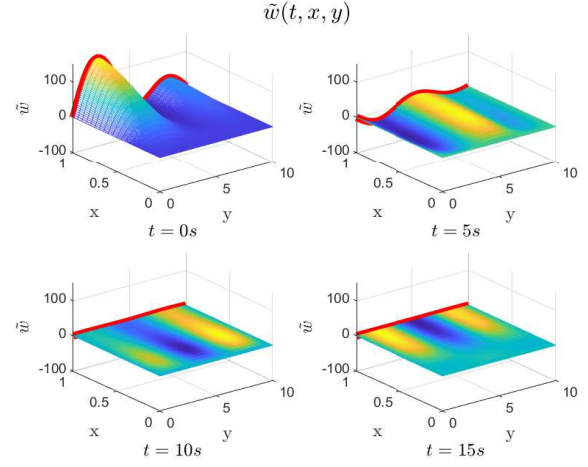


Fig. 6. Observer errors $\tilde{w}(t, x, y)$.

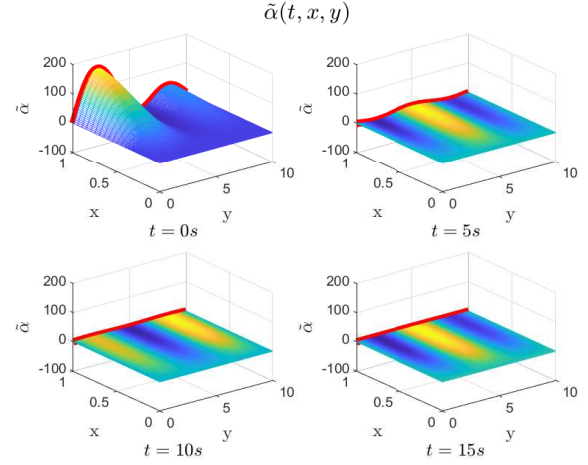


Fig. 7. Observer errors $\tilde{\alpha}(t, x, y)$.

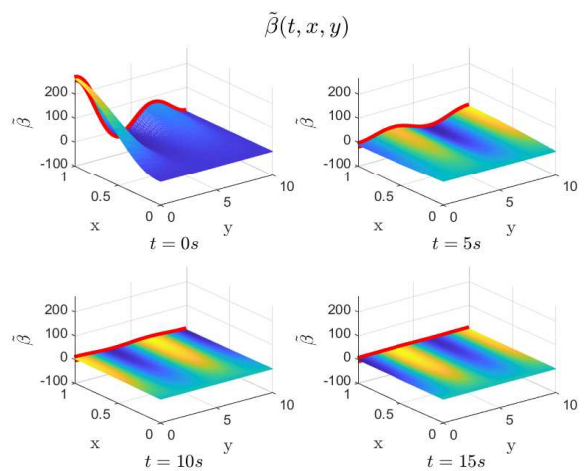


Fig. 8. Observer errors $\tilde{\beta}(t, x, y)$.

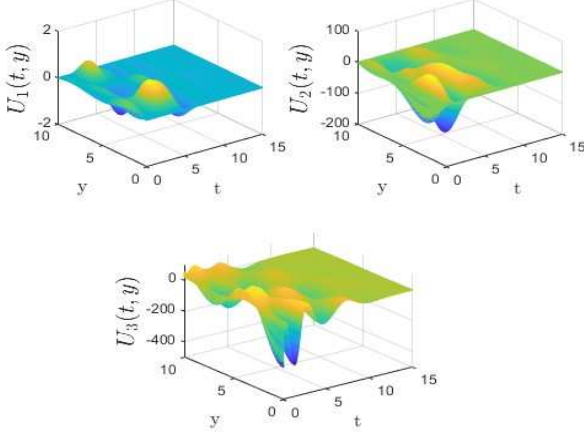


Fig. 9. Output-feedback control inputs.

7 Conclusion and Future Work

In this work, we modeled the flow-induced vibration of a two-dimensional elastic plate as a coupled system of two-dimensional wave PDEs with in-domain instabilities and designed a backstepping-based output-feedback boundary controller with anti-collocated boundary observer for active wing flutter suppression in high Mach number flight regimes. The two-dimensional control problem is decomposed into a series of one-dimensional modal systems via Fourier series expansion for control law design. The kernel equations were solved using a power-series approach, guaranteeing the exponential stability of the closed-loop system with a tunable convergence rate. Then, an anti-collocated boundary observer is constructed to recover the system states, ensuring the output-feedback control of the entire closed-loop system. Simulation results confirm that the proposed controller rapidly suppresses vibration instabilities, providing a systematic control framework for two-dimensional elastic structures with in-domain anti-damping sources. Future work will extend the design to adaptive control to address the system parameter uncertainties and external disturbances.

A Expression of the coefficients in (42)–(46)

The expressions of the coefficients in (42)–(46) are shown as follows.

$$\Sigma = \begin{bmatrix} \frac{1}{\sqrt{\epsilon}} & 0 & 0 \\ 0 & \frac{1}{\sqrt{\mu_1}} & 0 \\ 0 & 0 & \frac{1}{\sqrt{\mu_2}} \end{bmatrix}, A = \begin{bmatrix} 0 & -\frac{1}{\sqrt{\epsilon}} & 0 \\ 0 & 0 & \frac{n\pi}{L\sqrt{\mu_2}} \\ 0 & \frac{n\pi}{L\sqrt{\mu_2}} & 0 \end{bmatrix}, \quad (\text{A.1})$$

$$C = \begin{bmatrix} -1 & 0 & 0 \\ 0 & -1 & 0 \\ 0 & 0 & -1 \end{bmatrix}, D = \begin{bmatrix} 0 & 2 & 0 \\ 0 & 0 & 0 \\ 0 & -\frac{2n\pi}{L} & 0 \end{bmatrix},$$

$$F_{11}(x) = \begin{bmatrix} \frac{c_1(x)}{2} & c_2(x) & 0 \\ \frac{a(c_5(x)+c_6(x))}{4\epsilon\sqrt{\mu_1}} & 0 & -\frac{n\pi}{2L\sqrt{\mu_1}} \\ 0 & \frac{n\pi}{2L\sqrt{\mu_2}} & 0 \end{bmatrix},$$

$$\begin{aligned} F_{12}(x) &= \begin{bmatrix} -\frac{c_1(x)}{2} & 0 & 0 \\ \frac{a(c_5(x)-c_6(x))}{4\epsilon\sqrt{\mu_1}} & 0 & 0 \\ 0 & 0 & 0 \end{bmatrix}, \\ F_{21}(x) &= \begin{bmatrix} \frac{c_3(x)}{2} & c_4(x) & 0 \\ -\frac{a(c_5(x)+c_6(x))}{4\epsilon\sqrt{\mu_1}} & 0 & \frac{n\pi}{2L\sqrt{\mu_1}} \\ 0 & -\frac{n\pi}{2L\sqrt{\mu_2}} & 0 \end{bmatrix}, \\ F_{22}(x) &= \begin{bmatrix} \frac{c_3(x)}{2} & 0 & 0 \\ -\frac{a(c_5(x)-c_6(x))}{4\epsilon\sqrt{\mu_1}} & 0 & 0 \\ 0 & 0 & 0 \end{bmatrix}, \\ F_{13}(x) &= \begin{bmatrix} \frac{2n^2\pi^2}{L^2}c_2(x) & 0 & -\frac{2n\pi}{L}c_2(x) \\ 0 & -\frac{n^2\pi^2\epsilon+aL^2}{\epsilon L^2\sqrt{\mu_1}} & 0 \\ \frac{an\pi}{\epsilon L\sqrt{\mu_2}} & 0 & -\frac{n^2\pi^2\epsilon+aL^2}{\epsilon L^2\sqrt{\mu_2}} \end{bmatrix}, \\ F_{14}(x, y) &= \begin{bmatrix} -\frac{n^2\pi^2}{2\sqrt{\epsilon}L^2}f_{11}(x, y) & 0 & -\frac{n\pi}{L}c_2(x) \\ 0 & -\frac{n^2\pi^2\epsilon+aL^2}{2\epsilon L^2\sqrt{\mu_1}} & 0 \\ \frac{an\pi}{2\epsilon L\sqrt{\mu_2}}c_5(y) & 0 & -\frac{n^2\pi^2\epsilon+aL^2}{2\epsilon L^2\sqrt{\mu_2}} \end{bmatrix}, \\ F_{15}(x, y) &= \begin{bmatrix} -\frac{n^2\pi^2}{2\sqrt{\epsilon}L^2}f_{12}(x, y) & 0 & -\frac{n\pi}{L}c_2(x) \\ 0 & -\frac{n^2\pi^2\epsilon+aL^2}{2\epsilon L^2\sqrt{\mu_1}} & 0 \\ \frac{an\pi}{2\epsilon L\sqrt{\mu_2}}c_6(y) & 0 & -\frac{n^2\pi^2\epsilon+aL^2}{2\epsilon L^2\sqrt{\mu_2}} \end{bmatrix}, \\ F_{23}(x) &= \begin{bmatrix} \frac{2n^2\pi^2}{L^2}c_4(x) & 0 & -\frac{2n\pi}{L}c_4(x) \\ 0 & \frac{n^2\pi^2\epsilon+aL^2}{\epsilon L^2\sqrt{\mu_1}} & 0 \\ -\frac{an\pi}{\epsilon L\sqrt{\mu_2}} & 0 & \frac{n^2\pi^2\epsilon+aL^2}{\epsilon L^2\sqrt{\mu_2}} \end{bmatrix}, \\ F_{24}(x, y) &= \begin{bmatrix} \frac{n^2\pi^2}{2\sqrt{\epsilon}L^2}f_{21}(x, y) & 0 & -\frac{n\pi}{L}c_4(x) \\ 0 & \frac{n^2\pi^2\epsilon+aL^2}{2\epsilon L^2\sqrt{\mu_1}} & 0 \\ -\frac{an\pi}{2\epsilon L\sqrt{\mu_2}}c_5(y) & 0 & \frac{n^2\pi^2\epsilon+aL^2}{2\epsilon L^2\sqrt{\mu_2}} \end{bmatrix}, \\ F_{25}(x, y) &= \begin{bmatrix} \frac{n^2\pi^2}{2\sqrt{\epsilon}L^2}f_{22}(x, y) & 0 & -\frac{n\pi}{L}c_4(x) \\ 0 & \frac{n^2\pi^2\epsilon+aL^2}{2\epsilon L^2\sqrt{\mu_1}} & 0 \\ -\frac{an\pi}{2\epsilon L\sqrt{\mu_2}}c_6(y) & 0 & \frac{n^2\pi^2\epsilon+aL^2}{2\epsilon L^2\sqrt{\mu_2}} \end{bmatrix}, \end{aligned}$$

where $c_1(x) = \bar{c}_2 \exp(\sqrt{\epsilon}(\bar{c}_1 - \bar{c}_2)x)$, $c_2(x) = -\frac{1}{2\sqrt{\epsilon}} \times \exp(\sqrt{\epsilon}\bar{c}_1 x)$, $c_3(x) = -\bar{c}_1 \exp(-\sqrt{\epsilon}(\bar{c}_1 - \bar{c}_2)x)$, $c_4(x) = \frac{1}{2\sqrt{\epsilon}} \exp(\sqrt{\epsilon}\bar{c}_2 x)$, $c_5(x) = \exp(-\sqrt{\epsilon}\bar{c}_1 x)$, $c_6(x) = \exp(-\sqrt{\epsilon}\bar{c}_2 x)$, $f_{11}(x, y) = \exp(\sqrt{\epsilon}\bar{c}_1(x - y))$, $f_{12}(x, y) = \exp(\sqrt{\epsilon}(\bar{c}_1 x - \bar{c}_2 y))$, $f_{21}(x, y) = \exp(\sqrt{\epsilon}(\bar{c}_2 x - \bar{c}_1 y))$ and $f_{22}(x, y) = \exp(\sqrt{\epsilon}\bar{c}_2(x - y))$.

B Expression of $\mathcal{F}_{ij}(\xi)$ and \mathcal{D}_{ij}

For $i = 1, 2, 3$ and $j = 1, 2, 3, 4, 5, 6$, the functions $\mathcal{F}_{ij}(\xi)$ and \mathcal{D}_{ij} in (69)–(71) and (125)–(127) are shown as follows

$$\begin{aligned} \mathcal{F}_{i1}(\xi) &= \sqrt{\epsilon}\bar{c}_1 \exp(-\sqrt{\epsilon}\bar{c}_1\xi)k_{i1,n}(1, \xi) \\ &\quad + \sqrt{\epsilon}\bar{c}_2 \exp(-\sqrt{\epsilon}\bar{c}_2\xi)l_{i1,n}(1, \xi) \\ &\quad - \exp(-\sqrt{\epsilon}\bar{c}_1\xi)k_{i1,n,\xi}(1, \xi) \\ &\quad - \exp(-\sqrt{\epsilon}\bar{c}_2\xi)l_{i1,n,\xi}(1, \xi), \end{aligned} \quad (\text{B.1})$$

$$\begin{aligned} \mathcal{F}_{i2}(\xi) &= \sqrt{\epsilon} (\exp(-\sqrt{\epsilon}\bar{c}_1\xi)k_{i1,n}(1, \xi) \\ &\quad - \exp(-\sqrt{\epsilon}\bar{c}_2\xi)l_{i1,n}(1, \xi)), \end{aligned} \quad (\text{B.2})$$

$$\mathcal{F}_{i3}(\xi) = k_{i2,n,\xi}(1, \xi) + l_{i2,n,\xi}(1, \xi), \quad (\text{B.3})$$

$$\mathcal{F}_{i4}(\xi) = \sqrt{\mu} (k_{i2,n}(1, \xi) - l_{i2,n}(1, \xi)), \quad (\text{B.4})$$

$$\mathcal{F}_{i5}(\xi) = k_{i3,n,\xi}(1, \xi) + l_{i3,n,\xi}(1, \xi), \quad (\text{B.5})$$

$$\mathcal{F}_{i6}(\xi) = \sqrt{\mu} (k_{i3,n}(1, \xi) - l_{i3,n}(1, \xi)), \quad (\text{B.6})$$

$$\begin{aligned} \mathcal{D}_{i1} &= \exp(-\sqrt{\epsilon} \bar{c}_1) k_{i1,n}(1, 1) \\ &\quad + \exp(-\sqrt{\epsilon} \bar{c}_2) l_{i1,n}(1, 1), \end{aligned} \quad (\text{B.7})$$

$$\mathcal{D}_{i2} = k_{i1,n}(1, 0) + l_{i1,n}(1, 0) - \phi_{i1,n}(1), \quad (\text{B.8})$$

$$\mathcal{D}_{i4} = k_{i2,n}(1, 0) + l_{i2,n}(1, 0) - \phi_{i2,n}(1), \quad (\text{B.9})$$

$$\mathcal{D}_{i5} = k_{i3,n}(1, 1) + l_{i3,n}(1, 1), \quad (\text{B.10})$$

$$\mathcal{D}_{i6} = k_{i3,n}(1, 0) + l_{i3,n}(1, 0) - \phi_{i3,n}(1) \quad (\text{B.11})$$

with

$$\mathcal{D}_{13} = k_{12,n}(1, 1) + l_{12,n}(1, 1) - 1, \quad (\text{B.12})$$

$$\mathcal{D}_{23} = k_{22,n}(1, 1) + l_{22,n}(1, 1), \quad (\text{B.13})$$

$$\mathcal{D}_{33} = k_{32,n}(1, 1) + l_{32,n}(1, 1) + \frac{n\pi}{L}. \quad (\text{B.14})$$

C Proof of Theorem 1: Well-posedness of the Kernel Equations of K and L

To prove the well-posedness of the kernel equations, we classically transform the kernel equations into integral equations and use the method of successive approximations. For $1 \leq i, j \leq 3$, denote

$$\Lambda^+ = \Lambda^- = \Sigma, \quad Q_0 = C, \quad \Omega(x) = \{\omega_{ij}(x)\}, \quad (\text{C.1})$$

$$A = \{a_{ij}\}, \quad D = \{d_{ij}\}, \quad C = \{c_{ij}\}, \quad (\text{C.2})$$

$$\Sigma^{+}(x) = F_{11}(x) - F_{12}(x) = \{\sigma_{ij}^{+}(x)\}, \quad (\text{C.3})$$

$$\Sigma^{--}(x) = F_{11}(x) + F_{12}(x) = \{\sigma_{ij}^{--}(x)\}, \quad (\text{C.4})$$

$$\Sigma^{++}(x) = F_{21}(x) - F_{22}(x) = \{\sigma_{ij}^{++}(x)\}, \quad (\text{C.5})$$

$$\Sigma^{+-}(x) = F_{21}(x) + F_{22}(x) = \{\sigma_{ij}^{+-}(x)\}, \quad (\text{C.6})$$

$$F_{13}(x) = \{\varepsilon_{ij}^{++}(x)\}, \quad F_{23}(x) = \{\varepsilon_{ij}^{+-}(x)\}, \quad (\text{C.7})$$

$$F_{14}(x, y) = \{f_{ij}^{++}(x, y)\}, F_{15}(x, y) = \{f_{ij}^{+-}(x, y)\},$$

$$F_{24}(x, y) = \{f_{ij}^{-+}(x, y)\}, F_{25}(x, y) = \{f_{ij}^{--}(x, y)\}, \quad (\text{C.8})$$

$$F_{24}(x, y) = \{f_{ij}^{-+}(x, y)\}, F_{25}(x, y) = \{f_{ij}^{--}(x, y)\}, \quad (\text{C.9})$$

Developing Eqs. (49)–(55), and applying the method described in [20], we embed the ODE into the domain $\Gamma = \{0 \leq \xi \leq x \leq 1\}$ by denoting

$$I_{\{y=0\}}(x, y) = \begin{cases} 1 & \text{if } y = 0 \\ 0 & \text{otherwise.} \end{cases} \quad (\text{C.10})$$

Defining $\tilde{\phi}_{ij}$ such that $\forall (x, y) \in \Gamma, \tilde{\phi}_{ij}(x, y) = I_{\{y=0\}}(x, y) \phi_{ij}(x)$, we get the following set of kernel

PDEs:

for $1 \leq i \leq 3, 1 \leq j \leq 3$:

$$\begin{aligned} \lambda_i \partial_x L_{ij}(x, \xi) - \lambda_j \partial_\xi L_{ij}(x, \xi) &= \sum_{k=1}^3 \sigma_{kj}^{++}(\xi) L_{ik}(x, \xi) \\ &\quad + \sum_{p=1}^3 \sigma_{pj}^{--}(\xi) K_{ip}(x, \xi) - \sum_{i < p} L_{pj}(x, \xi) \omega_{ip}(x) \\ &\quad - f_{ij}^{+-}(x, \xi) + \int_\xi^x \sum_{p=1}^3 f_{pj}^{+-}(s, \xi) K_{ip}(x, s) ds \\ &\quad + \int_\xi^x \sum_{k=1}^3 f_{kj}^{--}(s, \xi) L_{ik}(x, s) ds, \end{aligned} \quad (\text{C.11})$$

$$\begin{aligned} \lambda_i \partial_x K_{ij}(x, \xi) + \lambda_j \partial_\xi K_{ij}(x, \xi) &= \sum_{k=1}^3 \sigma_{kj}^{--}(\xi) K_{ik}(x, \xi) \\ &\quad + \sum_{p=1}^3 \sigma_{pj}^{+-}(\xi) L_{ip}(x, \xi) - \sum_{i < p} K_{pj}(x, \xi) \omega_{ip}(x) \\ &\quad - f_{ij}^{++}(x, \xi) + \int_\xi^x \sum_{p=1}^3 f_{pj}^{++}(s, \xi) K_{ip}(x, s) ds \\ &\quad + \int_\xi^x \sum_{k=1}^3 f_{kj}^{+-}(s, \xi) L_{ik}(x, s) ds, \end{aligned} \quad (\text{C.12})$$

$$\begin{aligned} \lambda_i \partial_x \tilde{\phi}_{ij}(x, \xi) &= I_{\{\xi=0\}}(x, \xi) \left[\sum_{k=1}^3 a_{kj} \tilde{\phi}_{ik}(x, \xi) \right. \\ &\quad \left. + \sum_{p=1}^3 \lambda_p d_{pj} L_{ip}(x, 0) - \sum_{i < p} \omega_{ip}(x) \tilde{\phi}_{pj}(x, \xi) \right. \\ &\quad \left. - \varepsilon_{ij}^{++}(x) + \int_0^x \sum_{p=1}^3 \varepsilon_{pj}^{++}(x) K_{ip}(x, \xi) d\xi \right. \\ &\quad \left. + \int_0^x \sum_{k=1}^3 \varepsilon_{kj}^{+-}(x) L_{ik}(x, \xi) d\xi \right], \end{aligned} \quad (\text{C.13})$$

with the following set of boundary conditions

$\forall 1 \leq i, j \leq 3$:

$$L_{ij}(x, x) = -\frac{\sigma_{ij}^{--}(x)}{\lambda_i + \lambda_j} = l_{ij}(x), \quad (\text{C.14})$$

$$K_{ij}(x, x) = -\frac{\sigma_{ij}^{--}(x)}{\lambda_i - \lambda_j} = k_{ij}(x) \quad (j < i), \quad (\text{C.15})$$

$$\lambda_j k_{ij}(x, 0) = \sum_{k=1}^3 \lambda_k L_{ik}(x, 0) c_{kj} + \lambda_j \tilde{\phi}_{ij}(x, 0), \quad (\text{C.16})$$

$$\tilde{\phi}_{ij}(x, x) = I_{\{\xi=0\}}(x, x) \phi_{ij}(0). \quad (\text{C.17})$$

Besides, (53) imposes

$$\forall i \leq j, \quad \omega_{ij}(x) = (\lambda_i - \lambda_j) k_{ij}(x, x) + \sigma_{ij}^{--}(x). \quad (\text{C.18})$$

By induction, let us consider the following property $P(s)$ defined for all $1 \leq s \leq 3$:

For $\forall 1 \leq j \leq 3$ and $\forall 3 + 1 - s \leq i \leq 3$, the problem (C.11)–(C.18) has a unique solution $k_{ij}(\cdot, \cdot), l_{ij}(\cdot, \cdot), \tilde{\phi}_{ij}(\cdot, \cdot) \in L^\infty(\Gamma)$.

Let us assume that the property $P(s-1)$ ($1 < s \leq 3-1$) is true. We consequently have that $\forall 3 + 2 - s \leq p \leq 3$, $\forall 1 \leq j \leq 3$, $k_{pj}(\cdot, \cdot), l_{pj}(\cdot, \cdot)$, and $\tilde{\phi}_{pj}(\cdot, \cdot)$ are bounded. The proof follows along the line in [20] and [13] and is skipped due to space limitations. In the following we take $i = 3 + 1 - s$, we now show that (C.11)–(C.18) is well-posed and that $k_{ij}(\cdot, \cdot), l_{ij}(\cdot, \cdot), \tilde{\phi}_{ij}(\cdot, \cdot) \in L^\infty(\Gamma)$.

C.1 Method of Characteristics

C.1.1 Characteristics of the L kernels

For each $1 \leq i, j \leq 3$, and $(x, \xi) \in \Gamma$, we define the following characteristic lines $(x_{ij}(x, \xi; \cdot), \xi_{ij}(x, \xi; \cdot))$ corresponding to (C.11):

$$\begin{cases} \frac{dx_{ij}}{ds}(x, \xi; s) = -\lambda_i, & s \in [0, s_{ij}^F(x, \xi)] \\ x_{ij}(x, \xi; 0) = x, \quad x_{ij}(x, \xi; s_{ij}^F(x, \xi)) = x_{ij}^F(x, \xi) \end{cases} \quad (\text{C.19})$$

$$\begin{cases} \frac{d\xi_{ij}}{ds}(x, \xi; s) = \lambda_j, & s \in [0, s_{ij}^F(x, \xi)] \\ \xi_{ij}(x, \xi; 0) = \xi, \quad \xi_{ij}(x, \xi; s_{ij}^F(x, \xi)) = x_{ij}^F(x, \xi) \end{cases} \quad (\text{C.20})$$

These lines originate at the point (x, ξ) and terminate at the hypotenuse at the point $(x_{ij}^F(x, \xi), x_{ij}^F(x, \xi))$. Here, the expressions of $x_{ij}(x, \xi, s)$, $\xi_{ij}(x, \xi, s)$, $x_{ij}^F(x, \xi)$ and $s_{ij}^F(x, \xi)$, which are straightforward to obtain, are omitted for simplicity. Integrating (C.11) along the characteristic lines and plugging in the boundary condition (C.14) yields

$$\begin{aligned} L_{ij}(x, \xi) = & l_{ij}(x_{ij}^F) + \int_0^{s_{ij}^F(x, \xi)} \left[\sum_{k=1}^3 \sigma_{kj}^{++}(\xi_{ij}(x, \xi; s)) \right. \\ & \times L_{ik}(x_{ij}(x, \xi; s), \xi_{ij}(x, \xi; s)) \\ & + \sum_{p=1}^3 \sigma_{pj}^{-+}(\xi_{ij}(x, \xi; s)) K_{ip}(x_{ij}(x, \xi; s), \xi_{ij}(x, \xi; s)) \\ & - \sum_{i < p} L_{pj}(x_{ij}(x, \xi; s), \xi_{ij}(x, \xi; s)) ((\lambda_i - \lambda_p) \\ & \times K_{ip}(x_{ij}(x, \xi; s), \xi_{ij}(x, \xi; s)) + \sigma_{ip}^{--}(x_{ij}(x, \xi; s))) \\ & - f_{ij}^{+-}(x_{ij}(x, \xi; s), \xi_{ij}(x, \xi; s)) \\ & + f_{\xi_{ij}}^{x_{ij}} \sum_{p=1}^3 (f_{pj}^{+-}(\tau, \xi_{ij}(x, \xi; s)) K_{ip}(x_{ij}(x, \xi; s), \tau) \\ & \left. + f_{pj}^{--}(\tau, \xi_{ij}(x, \xi; s)) L_{ip}(x_{ij}(x, \xi; s), \tau)) d\tau \right] ds. \end{aligned} \quad (\text{C.21})$$

We can notice that the fourth line of (C.21) uses the expression of L_{pj} for $i < p$. This term is known and bounded (induction assumption).

C.1.2 Characteristics of the $\tilde{\phi}$ kernels

For each $1 \leq i, j \leq 3$, and $(x, \xi) \in \Gamma$, we define the following characteristic lines $(\kappa_{ij}(x, \xi; \cdot), \iota_{ij}(x, \xi; \cdot))$ corresponding to (C.13):

$$\begin{cases} \frac{d\kappa_{ij}}{d\eta}(x, \xi; \eta) = -\lambda_i, & \eta \in [0, \eta_{ij}^F(x, \xi)] \\ \kappa_{ij}(x, \xi; 0) = x, \quad \kappa_{ij}(x, \xi; \eta_{ij}^F(x, \xi)) = \xi \end{cases} \quad (\text{C.22})$$

$$\begin{cases} \frac{d\iota_{ij}}{d\eta}(x, \xi; \eta) = 0, & \eta \in [0, \eta_{ij}^F(x, \xi)] \\ \iota_{ij}(x, \xi; 0) = \xi, \quad \iota_{ij}(x, \xi; \eta_{ij}^F(x, \xi)) = \xi \end{cases} \quad (\text{C.23})$$

These lines originate at the point (x, ξ) and terminate at the hypotenuse at the point (ξ, ξ) . Integrating (C.13)

along the characteristic lines and plugging in the boundary condition (C.17) yields

$$\begin{aligned} \tilde{\phi}_{ij}(x, \xi) = & I_{\{\xi=0\}}(\xi, \xi) \phi_{ij}(0) \\ & + \int_0^{\eta_{ij}^F(x, \xi)} I_{\{\xi=0\}}(\kappa_{ij}(x, \xi; \eta), \iota_{ij}(x, \xi; \eta)) \\ & \left[\sum_{k=1}^3 a_{kj} \tilde{\phi}_{ik}(\kappa_{ij}(x, \xi; \eta), \iota_{ij}(x, \xi; \eta)) \right. \\ & + \sum_{p=1}^3 \lambda_p d_{pj} L_{ip}(\kappa_{ij}(x, \xi; \eta), 0) \\ & - \sum_{i < p} \tilde{\phi}_{pj}(\kappa_{ij}(x, \xi; \eta), \iota_{ij}(x, \xi; \eta)) \\ & \times ((\lambda_i - \lambda_p) K_{ip}(\kappa_{ij}(x, \xi; \eta), \iota_{ij}(x, \xi; \eta))) \\ & + \sigma_{ip}^{--}(\kappa_{ij}(x, \xi; \eta)) - \varepsilon_{ij}^{++}(\kappa_{ij}(x, \xi; \eta)) \\ & + \int_0^{\kappa_{ij}} \sum_{p=1}^3 (\varepsilon_{pj}^{++}(\kappa_{ij}(x, \xi; \eta)) K_{ip}(\kappa_{ij}(x, \xi; \eta), \tau) \\ & \left. + \varepsilon_{pj}^{+-}(\kappa_{ij}(x, \xi; \eta)) L_{ip}(\kappa_{ij}(x, \xi; \eta), \tau)) d\tau \right] d\eta. \end{aligned} \quad (\text{C.24})$$

The expressions of $\kappa_{ij}(x, \xi, s)$, $\iota_{ij}(x, \xi, s)$ and $\eta_{ij}^F(x, \xi)$, which are straightforward to obtain, are omitted here for simplicity. We can also notice that the fifth line of (C.24) uses the expression of $\tilde{\phi}_{pj}$ for $i < p$. This term is known and bounded (induction assumption).

C.1.3 Characteristics of the K kernels

For each $1 \leq i, j \leq 3$, and $(x, \xi) \in \Gamma$, we define the following characteristic lines $(\chi_{ij}(x, \xi; \cdot), \zeta_{ij}(x, \xi; \cdot))$ corresponding to (C.12):

$$\begin{cases} \frac{d\chi_{ij}}{d\nu}(x, \xi; \nu) = -\lambda_i, & \nu \in [0, \nu_{ij}^F(x, \xi)] \\ \chi_{ij}(x, \xi; 0) = x, \quad \chi_{ij}(x, \xi; \nu_{ij}^F(x, \xi)) = \chi_{ij}^F(x, \xi) \end{cases} \quad (\text{C.25})$$

$$\begin{cases} \frac{d\zeta_{ij}}{d\nu}(x, \xi; \nu) = -\lambda_j, & \nu \in [0, \nu_{ij}^F(x, \xi)] \\ \zeta_{ij}(x, \xi; 0) = \xi, \quad \zeta_{ij}(x, \xi; \nu_{ij}^F(x, \xi)) = \zeta_{ij}^F(x, \xi) \end{cases} \quad (\text{C.26})$$

These lines all originate from (x, ξ) and terminate either at the point $(\chi_{ij}^F(x, \xi), \chi_{ij}^F(x, \xi))$ or at the point $(\chi_{ij}^F(x, \xi), 0)$. They are three distinct cases $i < j$, $i = j$ and $i > j$. The detailed expressions of $\chi_{ij}(x, \xi, \nu)$, $\zeta_{ij}(x, \xi, \nu)$, $\chi_{ij}^F(x, \xi)$, $\zeta_{ij}^F(x, \xi)$ and $\nu_{ij}^F(x, \xi)$ are, again, omitted here because of space constrains. Integrating (C.12) along these characteristic lines, plugging in the boundary conditions (C.15), (C.16) and (C.21), (C.24) evaluated at $(\chi_{ij}^F(x, \xi), 0)$ yields

$$\begin{aligned} K_{ij}(x, \xi) = & -\delta_{ij} \frac{\sigma_{ij}^{--}(\chi_{ij}^F)}{\lambda_i - \lambda_j} + (1 - \delta_{ij}) \frac{1}{\lambda_j} \sum_{k=1}^3 \lambda_k c_{kj} l_{ik}(x_{ij}^F) \\ & + (1 - \delta_{ij}) \frac{1}{\lambda_j} \sum_{r=1}^3 \lambda_r c_{rj} \int_0^{s_{ir}^F(\chi_{ij}^F(x, \xi), 0)} \\ & \times \left[\sum_{k=1}^3 \sigma_{kr}^{++}(\xi_{ir}(\chi_{ij}^F(x, \xi), 0; s)) \right. \\ & \times L_{ik}(x_{ir}(\chi_{ij}^F(x, \xi), 0; s), \xi_{ir}(\chi_{ij}^F(x, \xi), 0; s)) \\ & + \sum_{k=1}^3 \sigma_{kr}^{+-}(\xi_{ir}(\chi_{ij}^F(x, \xi), 0; s)) \\ & \left. \times K_{ik}(x_{ir}(\chi_{ij}^F(x, \xi), 0; s), \xi_{ir}(\chi_{ij}^F(x, \xi), 0; s)) \right] \end{aligned}$$

$$\begin{aligned}
& -\sum_{i < p} L_{pr}(\chi_{ij}^F(x, \xi), 0; s), \xi_{ir}(\chi_{ij}^F(x, \xi), 0; s)) \\
& \times ((\lambda_i - \lambda_p) K_{ip}(x_{ir}(\chi_{ij}^F(x, \xi), 0; s), x_{ir}(\chi_{ij}^F(x, \xi), 0; s)) \\
& + \sigma_{ip}^{--}(\chi_{ij}^F(x, \xi), 0; s))) \\
& - f_{ir}^{+-}(x_{ir}(\chi_{ij}^F(x, \xi), 0; s), \xi_{ir}(\chi_{ij}^F(x, \xi), 0; s)) \\
& + f_{\xi_{ir}}^{x_{ir}} \sum_{p=1}^3 f_{pr}^{+-}(\tau, \xi_{ir}(\chi_{ij}^F(x, \xi), 0; s)) \\
& \times K_{ip}(x_{ir}(\chi_{ij}^F(x, \xi), 0; s), \tau) d\tau \\
& + f_{\xi_{ir}}^{x_{ir}} \sum_{k=1}^3 f_{kr}^{--}(\tau, \xi_{ir}(\chi_{ij}^F(x, \xi), 0; s)) \\
& \times L_{ik}(x_{ir}(\chi_{ij}^F(x, \xi), 0; s), \tau) d\tau] ds \\
& + (1 - \delta_{ij}) \phi_{ij}(0) + (1 - \delta_{ij}) \int_0^{\eta_{ij}^F(\chi_{ij}^F(x, \xi), 0)} \\
& \times \left[\sum_{k=1}^3 a_{kj} \tilde{\phi}_{ik}(\kappa_{ij}(\chi_{ij}^F(x, \xi), 0; \eta), \iota_{ij}(\chi_{ij}^F(x, \xi), 0; \eta)) \right. \\
& + \sum_{p=1}^3 \lambda_p d_{pj} L_{ip}(\kappa_{ij}(\chi_{ij}^F(x, \xi), 0; \eta), 0) \\
& - \sum_{i < p} \tilde{\phi}_{pj}(\kappa_{ij}(\chi_{ij}^F(x, \xi), 0; \eta), \iota_{ij}(\chi_{ij}^F(x, \xi), 0; \eta)) \\
& \times ((\lambda_i - \lambda_p) K_{ip}(\kappa_{ij}(\chi_{ij}^F(x, \xi), 0; \eta), \iota_{ij}(\chi_{ij}^F(x, \xi), 0; \eta)) \\
& + \sigma_{ip}^{--}(\kappa_{ij}(\chi_{ij}^F(x, \xi), 0; \eta))) - \varepsilon_{ij}^{++}(\kappa_{ij}(\chi_{ij}^F(x, \xi), 0; \eta)) \\
& + \int_0^{\kappa_{ij}} \sum_{p=1}^3 \varepsilon_{pj}^{++}(\kappa_{ij}(\chi_{ij}^F(x, \xi), 0; \eta)) \\
& \times K_{ip}(\kappa_{ij}(\chi_{ij}^F(x, \xi), 0; \eta), \tau) d\tau \\
& + \int_0^{\kappa_{ij}} \sum_{k=1}^3 \varepsilon_{kj}^{+-}(\kappa_{ij}(\chi_{ij}^F(x, \xi), 0; \eta)) \\
& \times L_{ik}(\kappa_{ij}(\chi_{ij}^F(x, \xi), 0; \eta), \tau) d\tau] d\eta \\
& + \int_0^{\nu_{ij}^F(x, \xi)} \left[\sum_{k=1}^3 \sigma_{kj}^{--}(\zeta_{ij}(x, \xi; \nu)) \right. \\
& \times K_{ik}(\chi_{ij}(x, \xi; \nu), \zeta_{ij}(x, \xi; \nu)) \\
& + \sum_{p=1}^3 \sigma_{pj}^{+-}(\zeta_{ij}(x, \xi; \nu)) L_{ip}(\chi_{ij}(x, \xi; \nu), \zeta_{ij}(x, \xi; \nu)) \\
& - \sum_{i < p} K_{pj}(\chi_{ij}(x, \xi; \nu), \zeta_{ij}(x, \xi; \nu)) \\
& \times ((\lambda_i - \lambda_p) K_{ip}(\chi_{ij}(x, \xi; \nu), \chi_{ij}(x, \xi; \nu)) \\
& + \sigma_{ip}^{--}(\chi_{ij}(x, \xi; \nu))) - f_{ij}^{++}(\chi_{ij}(x, \xi; \nu), \zeta_{ij}(x, \xi; \nu)) \\
& + \int_{\zeta_{ij}}^{\chi_{ij}} \sum_{p=1}^3 (f_{pj}^{++}(\tau, \zeta_{ij}(x, \xi; \nu)) K_{ip}(\chi_{ij}(x, \xi; \nu), \tau) \\
& \left. + f_{pj}^{--}(\tau, \zeta_{ij}(x, \xi; \nu)) L_{ip}(\chi_{ij}(x, \xi; \nu), \tau)) d\tau \right] d\nu, \tag{C.27}
\end{aligned}$$

where the coefficient $\delta_{ij}(x, \xi)$ is defined by

$$\delta_{ij}(x, \xi) = \begin{cases} 1 & \text{if } j < i \text{ and } \lambda_i \xi - \lambda_j x \geq 0 \\ 0 & \text{else.} \end{cases} \tag{C.28}$$

This coefficient reflects the fact that, as mentioned above, some characteristics terminate on the hypotenuse and others on the axis $\xi = 0$.

C.2 Method of successive approximations

We now use the method of successive approximations to solve (C.21), (C.24) and (C.27). Define first

$$\begin{aligned}
\forall 1 \leq i, j \leq 3, \quad \varphi_{ij}^1(x, \xi) &= l_{ij}(x_{ij}^F) \\
& + \int_0^{s_{ij}^F} \left[-\sum_{i < p} L_{pj}(x_{ij}(x, \xi; s), \xi_{ij}(x, \xi; s)) \right.
\end{aligned}$$

$$\times \sigma_{ip}^{--}(x_{ij}(x, \xi; s)) - f_{ij}^{+-}(x, \xi) \right] ds, \tag{C.29}$$

$$\begin{aligned}
\forall 1 \leq i, j \leq 3, \quad \varphi_{ij}^2(x, \xi) &= -\delta_{ij} \frac{\sigma_{ij}^{--}(\chi_{ij}^F)}{\lambda_i - \lambda_j} \\
& + (1 - \delta_{ij}) \frac{1}{\lambda_j} \sum_{k=1}^3 \lambda_k c_{kj} l_{ik}(x_{ij}^F) \\
& + (1 - \delta_{ij}) \frac{1}{\lambda_j} \sum_{r=1}^3 \lambda_r c_{rj} \int_0^{s_{ir}^F(\chi_{ij}^F(x, \xi), 0)} \\
& \times \left[-\sum_{i < p} L_{pr}(\chi_{ij}^F(x, \xi), 0; s), \xi_{ir}(\chi_{ij}^F(x, \xi), 0; s) \right. \\
& \times \sigma_{ip}^{--}(x_{ir}(\chi_{ij}^F(x, \xi), 0; s)) \\
& \left. - f_{ir}^{+-}(x_{ir}(\chi_{ij}^F(x, \xi), 0; s), \xi_{ir}(\chi_{ij}^F(x, \xi), 0; s)) \right] ds \\
& + (1 - \delta_{ij}) \phi_{ij}(0) + (1 - \delta_{ij}) \int_0^{\eta_{ij}^F(\chi_{ij}^F(x, \xi), 0)} \\
& \times \left[-\sum_{i < p} \tilde{\phi}_{pj}(\kappa_{ij}(\chi_{ij}^F(x, \xi), 0; \eta), \iota_{ij}(\chi_{ij}^F(x, \xi), 0; \eta)) \right. \\
& \times \sigma_{ip}^{--}(\kappa_{ij}(\chi_{ij}^F(x, \xi), 0; \eta)) \\
& - \varepsilon_{ij}^{++}(\kappa_{ij}(\chi_{ij}^F(x, \xi), 0; \eta))] d\eta + \int_0^{\nu_{ij}^F(x, \xi)} [\\
& - \sum_{i < p} K_{pj}(\chi_{ij}(x, \xi; \nu), \zeta_{ij}(x, \xi; \nu)) \sigma_{ip}^{--}(\chi_{ij}(x, \xi; \nu)) \\
& - f_{ij}^{++}(\chi_{ij}(x, \xi; \nu), \zeta_{ij}(x, \xi; \nu))] d\nu, \tag{C.30}
\end{aligned}$$

$$\begin{aligned}
\forall 1 \leq i, j \leq 3, \quad \varphi_{ij}^3(x, \xi) &= I_{\{\xi=0\}}(\xi, \xi) \phi_{ij}(0) \\
& - \int_0^{\eta_{ij}^F(x, \xi)} I_{\{\xi=0\}}(\kappa_{ij}(x, \xi; \eta), \iota_{ij}(x, \xi; \eta)) [\\
& \sum_{i < p} \tilde{\phi}_{pj}(\kappa_{ij}(x, \xi; \eta), \iota_{ij}(x, \xi; \eta)) \sigma_{ip}^{--}(\kappa_{ij}(x, \xi; \eta)) \\
& + \varepsilon_{ij}^{++}(\kappa_{ij}(x, \xi; \eta))] d\eta. \tag{C.31}
\end{aligned}$$

Besides, we define \vec{H} as the vector containing all the kernels as follows:

$$\begin{aligned}
\vec{H} &= \begin{bmatrix} L_{11} \cdots L_{33} & K_{11} \cdots K_{33} & \Phi_{11} \cdots \Phi_{33} \end{bmatrix}^\top, \\
\vec{\varphi} &= \begin{bmatrix} \varphi_{11}^1 \cdots \varphi_{33}^1 & \varphi_{11}^2 \cdots \varphi_{33}^2 & \varphi_{11}^3 \cdots \varphi_{33}^3 \end{bmatrix}^\top. \tag{C.32}
\end{aligned}$$

Consider the following linear operators acting on \vec{H} :

$$\forall 1 \leq i, j \leq 3 :$$

$$\begin{aligned}
\Psi_{ij}^1[\vec{H}](x, \xi) &= \int_0^{s_{ij}^F(x, \xi)} \left[\sum_{k=1}^3 \sigma_{kj}^{++}(\xi_{ij}(x, \xi; s)) \right. \\
& \times L_{ik}(x_{ij}(x, \xi; s), \xi_{ij}(x, \xi; s)) \\
& + \sum_{p=1}^3 \sigma_{pj}^{-+}(\xi_{ij}(x, \xi; s)) K_{ip}(x_{ij}(x, \xi; s), \xi_{ij}(x, \xi; s)) \\
& - \sum_{i < p} L_{pj}(x_{ij}(x, \xi; s), \xi_{ij}(x, \xi; s)) \\
& \times (\lambda_i - \lambda_p) K_{ip}(x_{ij}(x, \xi; s), \xi_{ij}(x, \xi; s)) \\
& + \int_{\xi_{ij}}^{x_{ij}} \sum_{p=1}^3 (f_{pj}^{++}(\tau, \xi_{ij}(x, \xi; \tau)) K_{ip}(x_{ij}(x, \xi; \tau), \tau) \\
& \left. + f_{pj}^{--}(\tau, \xi_{ij}(x, \xi; \tau)) L_{ip}(x_{ij}(x, \xi; \tau), \tau)) d\tau \right] ds, \tag{C.33}
\end{aligned}$$

$$\begin{aligned}
\Psi_{ij}^2[\vec{H}](x, \xi) &= (1 - \delta_{ij}) \frac{1}{\lambda_j} \sum_{r=1}^3 \lambda_r c_{rj} \int_0^{s_{ir}^F(\chi_{ij}^F(x, \xi), 0)} \\
& \times \left[\sum_{k=1}^3 \sigma_{kj}^{++}(\xi_{ir}(\chi_{ij}^F(x, \xi), 0; s)) \right. \\
& \times L_{ik}(x_{ir}(\chi_{ij}^F(x, \xi), 0; s), \xi_{ir}(\chi_{ij}^F(x, \xi), 0; s)) \\
& + \sum_{k=1}^3 \sigma_{kr}^{+-}(\xi_{ir}(\chi_{ij}^F(x, \xi), 0; s)) \\
& \times K_{ik}(x_{ir}(\chi_{ij}^F(x, \xi), 0; s), \xi_{ir}(\chi_{ij}^F(x, \xi), 0; s)) \\
& - \sum_{i < p} L_{pr}(\chi_{ij}^F(x, \xi), 0; s), \xi_{ir}(\chi_{ij}^F(x, \xi), 0; s)) \\
& \times (\lambda_i - \lambda_p) K_{ip}(x_{ir}(\chi_{ij}^F(x, \xi), 0; s), \xi_{ir}(\chi_{ij}^F(x, \xi), 0; s)) \\
& \left. + f_{ir}^{+-}(x_{ir}(\chi_{ij}^F(x, \xi), 0; s), \xi_{ir}(\chi_{ij}^F(x, \xi), 0; s)) \right] ds, \tag{C.34}
\end{aligned}$$

$$\begin{aligned}
& + \int_{\xi_{ir}}^{x_{ir}} \sum_{p=1}^3 f_{pr}^{+-}(\tau, \xi_{ir}(\chi_{ij}^F(x, \xi), 0; s)) \\
& \times K_{ip}(\chi_{ir}(\chi_{ij}^F(x, \xi), 0; s), \tau) d\tau \\
& + \int_{\xi_{ir}}^{x_{ir}} \sum_{k=1}^3 f_{kr}^{--}(\tau, \xi_{ir}(\chi_{ij}^F(x, \xi), 0; s)) \\
& \times L_{ik}(\chi_{ir}(\chi_{ij}^F(x, \xi), 0; s), \tau) d\tau \] ds \\
& + (1 - \delta_{ij}) \int_0^{\eta_{ij}^F(\chi_{ij}^F(x, \xi), 0)} \\
& \times \left[\sum_{k=1}^3 a_{kj} \tilde{\phi}_{ik}(\kappa_{ij}(\chi_{ij}^F(x, \xi), 0; \eta), \iota_{ij}(\chi_{ij}^F(x, \xi), 0; \eta)) \right. \\
& + \sum_{p=1}^3 \lambda_p d_{pj} L_{ip}(\kappa_{ij}(\chi_{ij}^F(x, \xi), 0; \eta), 0) \\
& - \sum_{i < p} \tilde{\phi}_{pj}(\kappa_{ij}(\chi_{ij}^F(x, \xi), 0; \eta), \iota_{ij}(\chi_{ij}^F(x, \xi), 0; \eta)) \\
& \times (\lambda_i - \lambda_p) K_{ip}(\kappa_{ij}(\chi_{ij}^F(x, \xi), 0; \eta), \iota_{ij}(\chi_{ij}^F(x, \xi), 0; \eta)) \\
& + \int_0^{\kappa_{ij}} \sum_{p=1}^3 \varepsilon_{pj}^{++}(\kappa_{ij}(\chi_{ij}^F(x, \xi), 0; \eta)) \\
& \times K_{ip}(\kappa_{ij}(\chi_{ij}^F(x, \xi), 0; \eta), \tau) d\tau \\
& + \int_0^{\kappa_{ij}} \sum_{k=1}^3 \varepsilon_{kj}^{+-}(\kappa_{ij}(\chi_{ij}^F(x, \xi), 0; \eta)) \\
& \times L_{ik}(\kappa_{ij}(\chi_{ij}^F(x, \xi), 0; \eta), \tau) d\tau \] d\eta + \int_0^{\nu_{ij}^F(x, \xi)} \\
& \left[\sum_{k=1}^3 \sigma_{kj}^{--}(\zeta_{ij}(x, \xi; \nu)) K_{ik}(\chi_{ij}(x, \xi; \nu), \zeta_{ij}(x, \xi; \nu)) \right. \\
& + \sum_{p=1}^3 \sigma_{pj}^{+-}(\zeta_{ij}(x, \xi; \nu)) L_{ip}(\chi_{ij}(x, \xi; \nu), \zeta_{ij}(x, \xi; \nu)) \\
& - \sum_{i < p} K_{pj}(\chi_{ij}(x, \xi; \nu), \zeta_{ij}(x, \xi; \nu)) \\
& \times (\lambda_i - \lambda_p) K_{ip}(\chi_{ij}(x, \xi; \nu), \chi_{ij}(x, \xi; \nu)) \\
& + \int_{\zeta_{ij}}^{\chi_{ij}} \left(\sum_{p=1}^3 f_{pj}^{++}(\tau, \zeta_{ij}(x, \xi; \nu)) K_{ip}(\chi_{ij}(x, \xi; \nu), \tau) \right. \\
& + \left. f_{pj}^{--}(\tau, \zeta_{ij}(x, \xi; \nu)) L_{ip}(\chi_{ij}(x, \xi; \nu), \tau) \right) d\tau \] d\nu, \quad (C.34) \\
& \Psi_{ij}^3[\vec{H}](x, \xi) = \int_0^{\eta_{ij}^F(x, \xi)} I_{\{\xi=0\}}(\kappa_{ij}(x, \xi; \eta), \iota_{ij}(x, \xi; \eta)) \\
& \left[\sum_{k=1}^3 a_{kj} \tilde{\phi}_{ik}(\kappa_{ij}(x, \xi; \eta), \iota_{ij}(x, \xi; \eta)) \right. \\
& + \sum_{p=1}^3 \lambda_p d_{pj} L_{ip}(\kappa_{ij}(x, \xi; \eta), 0) \\
& - \sum_{i < p} \tilde{\phi}_{pj}(\kappa_{ij}(x, \xi; \eta), \iota_{ij}(x, \xi; \eta)) \\
& \times (\lambda_i - \lambda_p) K_{ip}(\kappa_{ij}(x, \xi; \eta), \iota_{ij}(x, \xi; \eta)) \\
& + \int_0^{\kappa_{ij}} \sum_{p=1}^3 (\varepsilon_{pj}^{++}(\kappa_{ij}(x, \xi; \eta)) K_{ip}(\kappa_{ij}(x, \xi; \eta), \tau) \\
& + \left. \varepsilon_{pj}^{+-}(\kappa_{ij}(x, \xi; \eta)) L_{ip}(\kappa_{ij}(x, \xi; \eta), \tau) \right) d\tau \] d\eta. \quad (C.35)
\end{aligned}$$

Define then the following sequence:

$$\vec{H}^0(x, \xi) = 0, \quad (C.36)$$

$$\begin{aligned}
\vec{H}^q(x, \xi) &= \vec{\varphi} + \vec{\Psi}[\vec{H}^{q-1}](x, \xi) \\
&= \left[h_1 \dots h_9 h_{10} \dots h_{18} h_{19} \dots h_{27} \right]^\top. \quad (C.37)
\end{aligned}$$

where the expressions of the element in (C.37) are $h_1 = \varphi_{11}^1(x, \xi) + \Psi_{11}^1[\vec{H}^{q-1}](x, \xi)$, $h_9 = \varphi_{33}^1(x, \xi) + \Psi_{33}^1[\vec{H}^{q-1}](x, \xi)$, $h_{10} = \varphi_{11}^2(x, \xi) + \Psi_{11}^2[\vec{H}^{q-1}](x, \xi)$, $h_{18} = \varphi_{33}^2(x, \xi) + \Psi_{33}^2[\vec{H}^{q-1}](x, \xi)$, $h_{19} = \varphi_{11}^3(x, \xi) + \Psi_{11}^3[\vec{H}^{q-1}](x, \xi)$, $h_{27} = \varphi_{33}^3(x, \xi) + \Psi_{33}^3[\vec{H}^{q-1}](x, \xi)$.

One should notice that if the limit exists, then $\vec{H} = \lim_{q \rightarrow +\infty} \vec{H}^q(x, \xi)$ is a solution of the integral equations, and thus solves the original hyperbolic system. Besides, define for $q \geq 1$ the increment $\Delta \vec{H}^q = \vec{H}^q - \vec{H}^{q-1}$, with

$\Delta \vec{H}^0 = \vec{\varphi}$ by definition. Since the functional $\vec{\Psi}$ is linear, the following equation $\Delta \vec{H}^q(x, \xi) = \vec{\Psi}[\vec{H}^{q-1}](x, \xi)$ holds. Using the definition of $\Delta \vec{H}^q$, it follows that if the sum $\sum_{q=0}^{+\infty} \Delta \vec{H}^q(x, \xi)$ is finite, then:

$$\vec{H}(x, \xi) = \sum_{q=0}^{+\infty} \Delta \vec{H}^q(x, \xi). \quad (C.38)$$

C.3 Convergence of the successive approximation series

To prove convergence of the series, we look for a recursive upper bound, similarly to e.g., [21]. First, we define

$$\bar{\lambda} = \lambda_3, \bar{\lambda} = \frac{1}{\lambda_1}, \bar{\mu} = \max_{i,j} \{|\lambda_i - \lambda_p|\}, \quad (C.39)$$

$$\bar{a} = \max_{i,j} \{a_{ij}\}, \bar{d} = \max_{i,j} \{d_{ij}\}, \bar{c} = \max_{i,j} \{c_{ij}\}, \quad (C.40)$$

$$\bar{f} = \max_{i,j} \max_{(x, \xi) \in \Gamma} \{f_{ij}^{++}, f_{ij}^{+-}, f_{ij}^{-+}, f_{ij}^{--}\}, \quad (C.41)$$

$$\bar{\sigma} = \max_{i,j} \max_{x \in [0, 1]} \{\sigma_{ij}^{++}, \sigma_{ij}^{+-}, \sigma_{ij}^{-+}, \sigma_{ij}^{--}\}, \quad (C.42)$$

$$\bar{\varepsilon} = \max_{i,j} \max_{x \in [0, 1]} \{\varepsilon_{ij}^{++}(x), \varepsilon_{ij}^{+-}(x)\}. \quad (C.43)$$

and $\bar{S} = \max_{p > 1, 1 \leq j \leq n} \{ \|K_{pj}\|, \|L_{pj}\|, \|\tilde{\phi}_{pj}\| \}$, which is well-defined according to the hypothesis $P(s-1)$.

Claim 1 For $q \in \mathbb{N}$, $(x, \xi) \in \Gamma$ and $s_{ij}^F, \eta_{ij}^F, \nu_{ij}^F, x_{ij}(x, \xi; \cdot), \xi_{ij}(x, \xi; \cdot), \kappa_{ij}(x, \xi; \cdot), \iota_{ij}(x, \xi; \cdot), \chi_{ij}(x, \xi; \cdot), \zeta_{ij}(x, \xi; \cdot)$ defined as in (C.19), (C.20), (C.22), (C.23), (C.25) and (C.26), respectively, $\forall 1 \leq i, j \leq 3$, the following inequalities holds:

$$\int_0^{s_{ij}^F(x, \xi)} x_{ij}^q(x, \xi; s) ds \leq M_\lambda \frac{x^{q+1}}{q+1}, \quad (C.44)$$

$$\int_0^{\eta_{ij}^F(x, \xi)} \kappa_{ij}^q(x, \xi; \eta) ds \leq M_\lambda \frac{x^{q+1}}{q+1}, \quad (C.45)$$

$$\int_0^{\nu_{ij}^F(x, \xi)} \chi_{ij}^q(x, \xi; \nu) ds \leq M_\lambda \frac{x^{q+1}}{q+1}, \quad (C.46)$$

$$\text{where } M_\lambda = \max_{i=1,2,3} \left\{ \frac{1}{\lambda_i} \right\} = \frac{1}{\lambda_1}.$$

Proof. Consider the following change of integration variable, noting (C.19) and (C.20):

$$\tau = x_{ij}(x, \xi; s), \quad (C.47)$$

$$d\tau = \frac{d}{ds} x_{ij}(x, \xi; s) ds = -\lambda_i ds. \quad (C.48)$$

Thus, the left-hand-side of (C.44) rewrites:

$$\begin{aligned}
\int_0^{s_{ij}^F(x, \xi)} x_{ij}^q(x, \xi; s) ds &= \int_x^{x_{ij}^F(x, \xi)} \frac{-\tau^q}{\lambda_i} d\tau \\
&= \frac{x^{q+1} - (x_{ij}^F)^{q+1}}{\lambda_i (q+1)} \leq M_\lambda \frac{x^{q+1}}{q+1}. \quad (C.49)
\end{aligned}$$

Inequality (C.44) is obtained. Inequalities (C.45) and (C.46) are proved the same way using change of integration variables $\tau = \kappa_{ij}(x, \xi; \eta)$ and $\tau = \chi_{ij}(x, \xi; \nu)$. \square

Claim 2 For $q \geq 1$, assume that, for $\forall (x, \xi) \in \Gamma, \forall i = 1, \dots, 27$,

$$|\Delta \vec{H}_i^q(x, \xi)| \leq \bar{\varphi} \frac{M^q x^q}{q!}, \quad (\text{C.50})$$

where $\Delta \vec{H}_i^q(x, \xi)$ denotes the i -th ($i = 1, \dots, 27$) component of $\Delta \vec{H}^q(x, \xi)$, it follows that $\forall (x, \xi) \in \Gamma, \forall i = 1, 2, 3, \forall j = 1, 2, 3$:

$$|\Psi_{ij}^1[\Delta \vec{H}^q(x, \xi)]| \leq \bar{\varphi} \frac{M^{q+1} x^{q+1}}{(q+1)!}, \quad (\text{C.51})$$

$$|\Psi_{ij}^2[\Delta \vec{H}^q(x, \xi)]| \leq \bar{\varphi} \frac{M^{q+1} x^{q+1}}{(q+1)!}, \quad (\text{C.52})$$

$$|\Psi_{ij}^3[\Delta \vec{H}^q(x, \xi)]| \leq \bar{\varphi} \frac{M^{q+1} x^{q+1}}{(q+1)!}, \quad (\text{C.53})$$

where $M = [3\bar{\lambda}\underline{\lambda}\bar{c}(6\bar{\sigma} + 3\bar{\mu}\bar{S} + 3\bar{f}) + 3\bar{a} + 3\bar{\lambda}\bar{d} + 6\bar{\mu}\bar{S} + 6\bar{\varepsilon} + 6\bar{\sigma} + 6\bar{f}] \bar{\varphi} M_\lambda$.

Proof. Considering (C.50), using the expression of $\Psi_{ij}^1[\vec{H}](x, \xi)$ given by (C.33), for all $i = 1, \dots, 27$ and $(x, \xi) \in \Gamma$, one obtain

$$\begin{aligned} |\Psi_{ij}^1[\Delta \vec{H}^q](x, \xi)| &\leq \int_0^{s_{ij}^F(x, \xi)} \left| \sum_{k=1}^3 \sigma_{kj}^{++}(\xi_{ij}(x, \xi; s)) \right. \\ &\quad \times \Delta L_{ik}^q(x_{ij}(x, \xi; s), \xi_{ij}(x, \xi; s)) \\ &\quad + \sum_{p=1}^3 \sigma_{pj}^{-+}(\xi_{ij}(x, \xi; s)) \Delta K_{ip}^q(x_{ij}(x, \xi; s), \xi_{ij}(x, \xi; s)) \\ &\quad - \sum_{i < p} L_{pj}(x_{ij}(x, \xi; s), \xi_{ij}(x, \xi; s)) (\lambda_i - \lambda_p) \\ &\quad \times \Delta K_{ip}^q(x_{ij}(x, \xi; s), \xi_{ij}(x, \xi; s)) \\ &\quad + \int_{\xi_{ij}}^{x_{ij}} \sum_{p=1}^3 (f_{pj}^{+-}(\tau, \xi_{ij}(x, \xi; s)) \Delta K_{ip}^q(x_{ij}(x, \xi; s), \tau) \\ &\quad + f_{pj}^{--}(\tau, \xi_{ij}(x, \xi; s)) \Delta L_{ip}^q(x_{ij}(x, \xi; s), \tau)) d\tau \Big| ds, \end{aligned} \quad (\text{C.54})$$

using (C.44) and (C.50), which yields

$$\begin{aligned} |\Psi_{ij}^1[\Delta \vec{H}^q](x, \xi)| &\leq (6\bar{\sigma} + 3\bar{\mu}\bar{S}) \int_0^{s_{ij}^F(x, \xi)} \bar{\varphi} \frac{M^q x_{ij}(x, \xi; s)^q}{q!} ds \\ &\quad + 6\bar{f} \int_0^{s_{ij}^F(x, \xi)} \int_{\xi_{ij}}^{x_{ij}} \bar{\varphi} \frac{M^q x_{ij}(x, \xi; s)^q}{q!} d\tau ds \\ &= (6\bar{\sigma} + 3\bar{\mu}\bar{S} + 6\bar{f}) \int_0^{s_{ij}^F(x, \xi)} \bar{\varphi} \frac{M^q x_{ij}(x, \xi; s)^q}{q!} ds \\ &\leq (6\bar{\sigma} + 3\bar{\mu}\bar{S} + 6\bar{f}) \frac{\bar{\varphi} M_\lambda \frac{M^q x^{q+1}}{(q+1)!}}{q+1} \\ &\leq \bar{\varphi} \frac{M^{q+1} x^{q+1}}{(q+1)!}. \end{aligned} \quad (\text{C.55})$$

Similarly, for $1 \leq i, j \leq 3, (x, \xi) \in \Gamma$, one gets

$$\begin{aligned} &|\Psi_{ij}^2[\Delta \vec{H}^q](x, \xi)| \\ &\leq [3\bar{\lambda}\underline{\lambda}\bar{c}(6\bar{\sigma} + 3\bar{\mu}\bar{S}) + 3(\bar{a} + \bar{\lambda}\bar{d} + \bar{\mu}\bar{S}) + 3\bar{\lambda}\underline{\lambda}\bar{c} \cdot 6\bar{f} \\ &\quad + 6\bar{\varepsilon}] \cdot \bar{\varphi} M_\lambda \frac{M^q (\chi_{ij}^F(x, \xi))^{q+1}}{(q+1)!} \\ &\quad + (6\bar{\sigma} + 3\bar{\mu}\bar{S} + 6\bar{f}) \bar{\varphi} M_\lambda \frac{M^q x^{q+1}}{(q+1)!} \end{aligned} \quad (\text{C.56})$$

Using the fact that $\chi_{ij}^F(x, \xi) \leq x$, this yields

$$\begin{aligned} &|\Psi_{ij}^2[\Delta \vec{H}^q](x, \xi)| \\ &\leq [3\bar{\lambda}\underline{\lambda}\bar{c}(6\bar{\sigma} + 3\bar{\mu}\bar{S}) + 3(\bar{a} + \bar{\lambda}\bar{d} + \bar{\mu}\bar{S}) + 3\bar{\lambda}\underline{\lambda}\bar{c} \cdot 6\bar{f} \\ &\quad + 6\bar{\varepsilon} + 6\bar{\sigma} + 3\bar{\mu}\bar{S} + 6\bar{f}] \cdot \bar{\varphi} M_\lambda \frac{M^q x^{q+1}}{(q+1)!} \\ &= [3\bar{\lambda}\underline{\lambda}\bar{c}(6\bar{\sigma} + 3\bar{\mu}\bar{S} + 6\bar{f}) + 3\bar{a} + 3\bar{\lambda}\bar{d} + 6\bar{\mu}\bar{S} + 6\bar{\varepsilon} \\ &\quad + 6\bar{\sigma} + 6\bar{f}] \cdot \bar{\varphi} M_\lambda \frac{M^q x^{q+1}}{(q+1)!} \\ &\leq \bar{\varphi} \frac{M^{q+1} x^{q+1}}{(q+1)!}. \end{aligned} \quad (\text{C.57})$$

In the same way, for $1 \leq i, j \leq 3, (x, \xi) \in \Gamma$, using the fact that $\kappa_{ij}(x, \xi; \eta) \leq x$, one obtain

$$\begin{aligned} &|\Psi_{ij}^3[\Delta \vec{H}^q](x, \xi)| \\ &\leq (3\bar{a} + 3\bar{\lambda}\bar{d} + 3\bar{\mu}\bar{S} + 6\bar{\varepsilon}) \bar{\varphi} M_\lambda \frac{M^q x^{q+1}}{(q+1)!} \\ &\leq \bar{\varphi} \frac{M^{q+1} x^{q+1}}{(q+1)!}, \end{aligned} \quad (\text{C.58})$$

which concludes the proof. \square

Claim 2 directly leads to Theorem 1, and one has that the following series normally converges on Γ and we have the upper bound

$$|\vec{H}(x, \xi)| = \left| \sum_{q=0}^{+\infty} \Delta \vec{H}^q(x, \xi) \right| \leq \bar{\varphi} e^M. \quad (\text{C.59})$$

D Proof of Lemma 2: Well-posedness of the Kernel Equations of M and N

Developing Eqs.(102)–(106) we get the following set of kernel PDEs
for $1 \leq i, j \leq 3$

$$\begin{aligned} \lambda_i \partial_x M_{ij}(x, \xi) - \lambda_j \partial_\xi M_{ij}(x, \xi) &= \sum_{k=1}^3 \sigma_{ik}^{++}(x) M_{kj}(x, \xi) \\ &\quad + \sum_{p=1}^3 \sigma_{ip}^{+-}(x) N_{pj}(x, \xi) - \sum_{i < p} M_{ip}(x, \xi) \omega_{pj}(\xi) \\ &\quad + f_{ij}^{--}(x, \xi) + \int_\xi^x \sum_{p=1}^3 f_{ip}^{-+}(x, s) N_{pj}(s, \xi) ds \\ &\quad + \int_\xi^x \sum_{k=1}^3 f_{ik}^{--}(x, s) M_{kj}(s, \xi) ds, \end{aligned} \quad (\text{D.1})$$

$$\begin{aligned} \lambda_i \partial_x N_{ij}(x, \xi) + \lambda_j \partial_\xi N_{ij}(x, \xi) &= -\sum_{k=1}^3 \sigma_{ik}^{--}(x) N_{kj}(x, \xi) \\ &\quad - \sum_{p=1}^3 \sigma_{ip}^{-+}(x) M_{pj}(x, \xi) + \sum_{i < p} N_{ip}(x, \xi) \omega_{pj}(\xi) \\ &\quad - f_{ij}^{++}(x, \xi) - \int_\xi^x \sum_{p=1}^3 f_{ip}^{++}(x, s) N_{pj}(s, \xi) ds \\ &\quad - \int_\xi^x \sum_{k=1}^3 f_{ik}^{++}(x, s) M_{kj}(s, \xi) ds, \end{aligned} \quad (\text{D.2})$$

with the following set of boundary conditions for $\forall 1 \leq i, j \leq 3$:

$$M_{ij}(x, x) = \frac{\sigma_{ij}^{+-}}{\lambda_i + \lambda_j}, \quad (D.3)$$

$$N_{ij}(x, x) = -\frac{\sigma_{ij}^{--}}{\lambda_i - \lambda_j}, \quad (j < i) \quad (D.4)$$

$$\omega_{ij}(x) = (\lambda_i - \lambda_j)N_{ij}(x, x) + \sigma_{ij}^{--}(x) \quad (j < i), \quad (D.5)$$

where the definition of λ_i , σ_{ij}^{++} , σ_{ij}^{+-} , σ_{ij}^{-+} , σ_{ij}^{--} , ω_{ij} , f_{ij}^{++} , f_{ij}^{+-} , f_{ij}^{-+} and f_{ij}^{--} are shown in Appendix-C. Evaluating (100), (101) at $x = 1$ yields

$$\forall 1 \leq i, j \leq 3, \quad N_{ij}(1, x) = r_i M_{ij}(1, x), \quad (D.6)$$

where r_i denotes the (i, i) -th (diagonal) entry of matrix R , and d_{ij}^+ , d_{ij}^- are given by

$$d_{ij}^+(x, \xi) = -\sum_{k=1}^3 M_{ik}(x, \xi) \sigma_{kj}^{-+}(y) - \int_{\xi}^x \sum_{k=1}^3 M_{ik}(s, \xi) d_{kj}^-(s, \xi) ds + f_{ij}^{--}(x, \xi), \quad (D.7)$$

$$d_{ij}^-(x, \xi) = -\sum_{k=1}^3 N_{ik}(x, \xi) \sigma_{kj}^{-+}(y) - \int_{\xi}^x \sum_{k=1}^3 N_{ik}(s, \xi) d_{kj}^-(s, \xi) ds + f_{ij}^{+-}(x, \xi), \quad (D.8)$$

provided the M and N kernels are well-defined. Finally, the observer gains are given by

$$p_{ij}^+(x) = \lambda_j m_{ij}(x, 0), \quad p_{ij}^-(x) = \lambda_j n_{ij}(x, 0). \quad (D.9)$$

Indeed, considering the following alternate variables

$$\bar{M}_{ij}(\chi, y) = M_{ij}(1 - y, 1 - \chi) = M_{ij}(x, \xi), \quad (D.10)$$

$$\bar{N}_{ij}(\chi, y) = N_{ij}(1 - y, 1 - \chi) = N_{ij}(x, \xi), \quad (D.11)$$

$$\bar{\omega}_{ij}(y) = \omega_{ij}(\xi), \quad (D.12)$$

$$\bar{f}_{ij}^{++}(\chi, y) = f_{ij}^{++}(1 - y, 1 - \chi) = f_{ij}^{++}(x, \xi), \quad (D.13)$$

$$\bar{f}_{ij}^{+-}(\chi, y) = f_{ij}^{+-}(1 - y, 1 - \chi) = f_{ij}^{+-}(x, \xi), \quad (D.14)$$

$$\bar{f}_{ij}^{-+}(\chi, y) = f_{ij}^{-+}(1 - y, 1 - \chi) = f_{ij}^{-+}(x, \xi), \quad (D.15)$$

$$\bar{f}_{ij}^{--}(\chi, y) = f_{ij}^{--}(1 - y, 1 - \chi) = f_{ij}^{--}(x, \xi), \quad (D.16)$$

$$\bar{\sigma}_{ij}^{++}(\chi) = \sigma_{ij}^{++}(x), \quad \bar{\sigma}_{ij}^{+-}(\chi) = \sigma_{ij}^{+-}(x), \quad (D.17)$$

$$\bar{\sigma}_{ij}^{-+}(\chi) = \sigma_{ij}^{-+}(x), \quad \bar{\sigma}_{ij}^{--}(\chi) = \sigma_{ij}^{--}(x), \quad (D.18)$$

one can prove that this system has the same structure as the controller kernel system in Appendix-C, but differs in the absence of ODE, which does not affect the overall proof process. Using a similar proof, we can obtain its well-posedness.

E Proof of Lemma 1: Lyapunov-Based Stability Analysis

In this section, we use a Lyapunov function for the stability analysis of the target system for each mode n , to show exponential stability of the origin with a tunable

convergence rate. For convenience, we will omit the subscript n in the proof. Define

$$V = \zeta_1 X^T X + \zeta_2 \int_0^1 e^{\delta x} \sigma^T(t, x) \Sigma^{-1} \sigma(t, x) dx + \int_0^1 e^{-\delta x} \psi^T(t, x) \Sigma^{-1} \psi(t, x) dx. \quad (E.1)$$

Differentiating (E.1) with respect to t , we get

$$\dot{V} = 2\zeta_1 X^T X_t + 2\zeta_2 \int_0^1 e^{\delta x} \sigma^T(t, x) \Sigma^{-1} \sigma_t(t, x) dx + 2 \int_0^1 e^{-\delta x} \psi^T(t, x) \Sigma^{-1} \psi_t(t, x) dx. \quad (E.2)$$

Recalling (62), E_1 has the following expression:

$$E_1 = \Sigma \Phi(0) + A, \quad (E.3)$$

we choose the boundary conditions $\Phi(0)$ according to (55) with $\delta_1, \delta_2, \delta_3 > 0$, then E_1 is a diagonal matrix with entries $-\delta_1, -\delta_2$ and $-\delta_3$. Choosing parameter $c = \min\{\delta_1, \delta_2, \delta_3\}$, we have $X^T E_1 X \leq -c X^T X$. Substituting (58)–(61) into (E.2), we have

$$\begin{aligned} \dot{V} \leq & -2\zeta_1 c X^T X + 2\zeta_1 X^T \Sigma \sigma(t, 0) - \zeta_2 \sigma^T(t, 0) \sigma(t, 0) \\ & - \zeta_2 \int_0^1 e^{\delta x} \sigma^T(t, x) (\delta I - 2\Sigma^{-1} \Omega(x)) \sigma(t, x) dx \\ & - \int_0^1 e^{-\delta x} \psi^T(t, x) (\delta I - 2\Sigma^{-1} (F_{21}(x) - F_{22}(x))) \psi(t, x) dx \\ & + 2 \int_0^1 e^{-\delta x} \psi^T(t, x) \Sigma^{-1} \int_0^x \Xi_2(x, y) \sigma(t, y) dy dx \\ & + 2 \int_0^1 e^{-\delta x} \psi^T(t, x) \Sigma^{-1} \int_0^x \Xi_3(x, y) \psi(t, y) dy dx \\ & + 2 \int_0^1 e^{-\delta x} \psi^T(t, x) \Sigma^{-1} ((F_{21}(x) + F_{22}(x)) \sigma(t, x) \\ & + \Xi_1(x) X) dx + \psi^T(t, 0) \psi(t, 0). \end{aligned} \quad (E.4)$$

Regarding the last term of (E.4), using $\psi(t, 0) = E_2 X + C \sigma(t, 0)$, we have $\psi^T(t, 0) \psi(t, 0) = X^T E_2^T E_2 X + 2X^T E_2^T C \sigma(t, 0) + \sigma^T(t, 0) C^T C \sigma(t, 0)$. Then, the first line and last term of (E.4) become

$$\begin{aligned} & -X^T (2\zeta_1 c I - E_2^T E_2) X + 2X^T (\zeta_1 \Sigma + E_2^T C) \sigma(t, 0) \\ & - \sigma^T(t, 0) (\zeta_2 I - C^T C) \sigma(t, 0) \\ & \leq -(2\zeta_1 c - M_1) X^T X - (\zeta_2 - M_2) \sigma^T(t, 0) \sigma(t, 0), \end{aligned} \quad (E.5)$$

with $M_1 = \|E_2\|^2 + 1$, $M_2 = \|\zeta_1 \Sigma + E_2^T C\|^2 + \|C\|^2$. The sixth line of (E.4) is bounded as follows:

$$\begin{aligned} & 2 \int_0^1 e^{-\delta x} \psi^T(t, x) \Sigma^{-1} ((F_{21}(x) + F_{22}(x)) \sigma(t, x) \\ & + \Xi_1(x) X) dx \\ & \leq (1 + M_4) \int_0^1 e^{-\delta x} \psi^T(t, x) \psi(t, x) dx \\ & + M_3 \int_0^1 e^{\delta x} \sigma^T(t, x) \sigma(t, x) dx + X^T X, \end{aligned} \quad (E.6)$$

with $M_3 = \max_{x \in [0, 1]} \|\Sigma^{-1} (F_{21}(x) + F_{22}(x))\|^2$ and $M_4 = \max_{x \in [0, 1]} \|\Sigma^{-1} \Xi_1(x)\|^2$. The fourth line of (E.4)

is bounded as follows:

$$\begin{aligned} & 2 \int_0^1 e^{-\delta x} \psi^\top(t, x) \Sigma^{-1} \int_0^x \Xi_2(x, y) \sigma(t, y) dy dx \\ & \leq \int_0^1 e^{-\delta x} \psi^\top(t, x) \psi(t, x) dx \\ & + M_5 \int_0^1 e^{\delta x} \sigma^\top(t, x) \sigma(t, x) dx, \end{aligned} \quad (\text{E.7})$$

with $M_5 = \max_{x, y \in [0, 1]} \|\Sigma^{-1} \Xi_2(x, y)\|^2$. The fifth line of (E.4) is also bounded:

$$\begin{aligned} & 2 \int_0^1 e^{-\delta x} \psi^\top(t, x) \Sigma^{-1} \int_0^x \Xi_3(x, y) \psi(t, y) dy dx \\ & \leq M_6 \int_0^1 e^{-\delta x} \psi^\top(t, x) \psi(t, x) dx, \end{aligned} \quad (\text{E.8})$$

with $M_6 = 1 + \max_{x, y \in [0, 1]} \|\Sigma^{-1} \Xi_3(x, y)\|^2$. Thus,

$$\begin{aligned} \dot{V}_1 & \leq -(2\zeta_1 c - M_1 - 1) X^\top X - (\zeta_2 - M_2) \sigma^\top(t, 0) \sigma(t, 0) \\ & - \int_0^1 e^{\delta x} \sigma^\top(t, x) (\zeta_2 \delta I - 2\zeta_2 \Sigma^{-1} \Omega(x) \\ & - M_3 I - M_5 I) \sigma(t, x) dx \\ & + \int_0^1 e^{-\delta x} \psi^\top(t, x) (M_6 I + 2\Sigma^{-1} (F_{21}(x) - F_{22}(x)) \\ & + 2I + M_4 I - \delta I) \psi(t, x) dx. \end{aligned} \quad (\text{E.9})$$

If we choose parameters:

$$c = (c' + 1)/2, \zeta_1 = M_1 + 1, \quad (\text{E.10})$$

$$\begin{aligned} \delta & > \max\{(2 \max_{x \in [0, 1]} \|F_{21}(x) - F_{22}(x)\| + c') \|\Sigma^{-1}\| + M_6 \\ & + M_4 + 2, (c' + 2 \max_{x \in [0, 1]} \|\Omega(x)\|) \|\Sigma^{-1}\| + 1\}, \end{aligned} \quad (\text{E.11})$$

$$\zeta_2 > \max\{M_3 + M_5, M_2\}, \quad (\text{E.12})$$

with $c' = 2 \min\{\delta_1, \delta_2, \delta_3\} - 1 > 0$, one can obtain

$$\begin{aligned} \dot{V} & \leq -c' \zeta_1 X^\top X - c' \zeta_2 \int_0^1 e^{\delta x} \sigma^\top(t, x) \Sigma^{-1} \sigma(t, x) dx \\ & - c' \int_0^1 e^{-\delta x} \psi^\top(t, x) \Sigma^{-1} \psi(t, x) dx \\ & \leq -c' V. \end{aligned} \quad (\text{E.13})$$

Recalling both direct transformation (47)–(48) and inverse transformation (64)–(65), and applying Cauchy-Schwarz inequality, we obtain

$$\begin{aligned} & \|p(t, \cdot)\|_{L^2}^2 + \|q(t, \cdot)\|_{L^2}^2 + \|r(t, \cdot)\|_{L^2}^2 + \|s(t, \cdot)\|_{L^2}^2 \\ & + \|u(t, \cdot)\|_{L^2}^2 + \|v(t, \cdot)\|_{L^2}^2 + x_1^2(t) + x_2^2(t) + x_3^2(t) \\ & \leq K e^{-c't} (\|p_0\|_{L^2}^2 + \|q_0\|_{L^2}^2 + \|r_0\|_{L^2}^2 + \|s_0\|_{L^2}^2 \\ & + \|u_0\|_{L^2}^2 + \|v_0\|_{L^2}^2 + x_1^2(0) + x_2^2(0) + x_3^2(0)) \end{aligned} \quad (\text{E.14})$$

for some positive K . Considering

$$\left\{ \begin{array}{l} \alpha_n(t, x) = \frac{1}{2} [\int_0^x (r_n(t, y) + s_n(t, y)) dy + 2x_2(t)], \\ \beta_n(t, x) = \frac{1}{2} [\int_0^x (u_n(t, y) + v_n(t, y)) dy + 2x_3(t)], \\ w_n(t, x) = \int_0^x \frac{k_2(y)p_n(t, y) + k_1(y)q_n(t, y)}{k_1(y) \cdot k_2(y)} dy + x_1(t), \\ \alpha_{n,t}(t, x) = \frac{r_n(t, x) - s_n(t, x)}{2\sqrt{\mu_1}}, \beta_{n,t}(t, x) = \frac{u_n(t, x) - v_n(t, x)}{2\sqrt{\mu_2}}, \\ w_{n,t}(t, x) = \frac{k_2(x)p_n(t, x) - k_1(x)q_n(t, x)}{2\sqrt{\epsilon(k_1(x) \cdot k_2(x))}}, \\ \alpha_{n,x}(t, x) = \frac{r_n(t, x) + s_n(t, x)}{2}, \beta_{n,x}(t, x) = \frac{u_n(t, x) + v_n(t, x)}{2}, \\ w_{n,x}(t, x) = \frac{k_2(x)p_n(t, x) + k_1(x)q_n(t, x)}{2k_1(x) \cdot k_2(x)}, \end{array} \right. \quad (\text{E.15})$$

which are obtained from (36)–(40), where functions $k_1(x) = \exp(\sqrt{\epsilon} \bar{c}_1 x)$, $k_2(x) = \exp(\sqrt{\epsilon} \bar{c}_2 x)$, we thus obtain this lemma.

References

- [1] J. Auriol, N. Kazemi, R. J. Shor, K. A. Innanen, and I. D. Gates. A sensing and computational framework for estimating the seismic velocities of rocks interacting with the drill bit. In *IEEE Trans. Geosci. Remote Sens.*, volume 58, pages 3178–3189, 2020.
- [2] J. Auriol and F. D. Meglio. Minimum time control of heterodirectional linear coupled hyperbolic pdes. *Automatica*, 71:300–307, 2016.
- [3] B. Bamieh, F. Paganini, and M. A. Dahleh. Distributed control of spatially invariant systems. *IEEE Trans. Autom. Control*, 47(7):1091–1107, 2002.
- [4] A. Bouhamed, A. Elkabouss, P. P. de Carvalho, and H. Bouzahir. Boundary optimal control problem of semi-linear kirchhoff plate equation. *Nonlinear Anal. Real World Appl.*, 80:104146, 2024.
- [5] D. Bresch-Pietri and M. Krstic. Adaptive output feedback for oil drilling stick-slip instability modeled by wave pde with anti-damped dynamic boundary. In *2014 American Control Conference*, pages 386–391, 2014.
- [6] D. Bresch-Pietri and M. Krstic. Adaptive output-feedback for wave pde with anti-damping - application to surface-based control of oil drilling stick-slip instability. In *53rd IEEE Conference on Decision and Control*, pages 1295–1300, 2014.
- [7] G. W. Chen, R. Vazquez, and M. Krstic. Rapid stabilization of timoshenko beam by pde backstepping. *IEEE Trans. Autom. Control*, 69(2):1141–1148, 2024.
- [8] J. M. Coron, R. Vazquez, M. Krstic, and G. Bastin. Local exponential H^2 stabilization of a 2d quasilinear hyperbolic system using backstepping. *SIAM J. Control Optim.*, 51(3):2005–2035, 2013.
- [9] E. H. Dowell and K. C. Hall. Modeling of fluid-structure interaction. *Annu. Rev. Fluid Mech.*, 33(1):445–490, 2001.
- [10] D. Guan, Y. Chen, J. Qi, and L. Du. Bilateral boundary control of an input delayed 2-d reaction-diffusion equation. *Automatica*, 157:111242, 2023.
- [11] D. Guan and J. Qi. Bilateral control for an unstable 2-d reaction-diffusion equation with unequal input delays at the boundaries. *IFAC-PapersOnLine*, 59(8):255–260, 2025.

[12] S. M. Han, H. Benaroya, and T. Wei. Dynamics of transversely vibrating beams using four engineering theories. *J. Sound Vib.*, 225(5):935–988, 1999.

[13] L. Hu, F. D. Meglio, R. Vazquez, and M. Krstic. Control of homodirectional and general heterodirectional linear coupled hyperbolic pdes. *IEEE Trans. Autom. Control*, 61(11):3301–3314, 2016.

[14] J. Deutscher. Finite-time output regulation for linear 2×2 hyperbolic systems using backstepping. *Automatica*, 75:54–62, 2017.

[15] M. Krstic, B. Z. Guo, A. Balogh, and A. Smyshlyaev. Control of a tip-force destabilized shear beam by observer-based boundary feedback. *SIAM J. Control Optim.*, 47(2):553–574, 2008.

[16] M. Krstic, A. A. Siranosian, and A. Smyshlyaev. Backstepping boundary controllers and observers for the slender timoshenko beam: Part i - design. In *2006 American Control Conference*, pages 2412–2417, 2006.

[17] J. E. Lagnese. *Boundary stabilization of thin plates*. SIAM, 1989.

[18] W. Littman and L. Markus. Stabilization of a hybrid system of elasticity by feedback boundary damping. *Ann. Mat. Pura Appl.*, 152:281–330, 1988.

[19] Y. Liu, W. Jiang, and F. Huang. On the stabilization of elastic plates with dynamical boundary control. *Appl. Math. Lett.*, 18(3):353–359, 2005.

[20] F. D. Meglio, F. B. Argomedo, L. Hu, and M. Krstic. Stabilization of coupled linear heterodirectional hyperbolic pde-ode systems. *Automatica*, 87:281–289, 2018.

[21] F. D. Meglio, R. Vazquez, and M. Krstic. Stabilization of a system of $n+1$ coupled first-order hyperbolic linear pdes with a single boundary input. *IEEE Trans. Autom. Control*, 58(12):3097–3111, 2013.

[22] C. Mittelstedt. *Theory of Plates and Shells*. Springer Vieweg Berlin, Heidelberg, 1 edition, May 2023.

[23] J. Qi, R. Vazquez, and M. Krstic. Multi-agent deployment in 3-d via pde control. *IEEE Trans. Autom. Control*, 60(4):891–906, 2015.

[24] A. Smyshlyaev and M. Krstic. Boundary control of an anti-stable wave equation with anti-damping on the uncontrolled boundary. *Systems & Control Letters*, 58(8):617–623, 2009.

[25] R. Vazquez, G. W. Chen, J. F. Qiao, and M. Krstic. The power series method to compute backstepping kernel gains: Theory and practice. In *Proc. 2023 62nd IEEE Conf. Decis. Control (CDC)*, pages 8162–8169, 2023.

[26] R. Vazquez and M. Krstic. A closed-form feedback controller for stabilization of the linearized 2-d navier–stokes poiseuille system. *IEEE Trans. Autom. Control*, 52(12):2298–2312, 2007.

[27] R. Vazquez and M. Krstic. Boundary observer for output-feedback stabilization of thermal-fluid convection loop. *IEEE Trans. Control Syst. Technol.*, 18(4):789–797, 2009.

[28] R. Vazquez and M. Krstic. Explicit output-feedback boundary control of reaction-diffusion pdes on arbitrary-dimensional balls. *Proc. IEEE Eur. Control Conf.*, pages 879–884, 2015.

[29] R. Vazquez and M. Krstic. Boundary control of a singular reaction-diffusion equation on a disk. *IFAC-PapersOnLine*, 49(8):74–79, 2016.

[30] R. Vazquez and M. Krstic. Boundary control of reaction-diffusion pdes on balls in spaces of arbitrary dimensions. *ESAIM: Control Optim. Calc. Var.*, 22(4):1078–1096, 2016.

[31] R. Vazquez and M. Krstic. Boundary control and estimation of reaction–diffusion equations on the sphere under revolution symmetry conditions. *Int. J. Control.*, 2019.

[32] R. Vazquez, M. Krstic, and J. M. Coron. Backstepping boundary stabilization and state estimation of a 2×2 linear hyperbolic system. *Proc. 50th Conf. Decis. Control Eur. Control Conf.*, pages 4937–4942, 2011.

[33] R. Vazquez, M. Krstic, J. Zhang, and J. Qi. Stabilization of a 2-d reaction-diffusion equation with a coupled pde evolving on its boundary. *Proc. 2019 IEEE Conf. Decis. Control (CDC)*, 2019.

[34] Chengyi Wang and Ji Wang. Output-Feedback Boundary Control of Thermally and Flow-Induced Vibrations in Slender Timoshenko Beams. *arXiv e-prints*, page arXiv:2503.21281, 2025.

[35] J. Wang, S. Koga, Y. Pi, and M. Krstic. Axial vibration suppression in a partial differential equation model of ascending mining cable elevator. *J. Dyn. Syst. Meas. Control*, 140(11):111003, 2018.

[36] J. Wang and M. Krstic. Vibration suppression for coupled wave pdes in deep-sea construction. *IEEE Trans. Control Syst. Technol.*, 29(4):1733–1749, 2020.

[37] J. Wang and M. Krstic. *PDE control of string-actuated motion*. Princeton University Press, 2022.

[38] S. Wang, M. Diagne, and J. Qi. Delay-adaptive compensation for 3-d formation control of leader-actuated multi-agent systems. *Automatica*, 164:111645, 2024.

[39] C. Xu, E. Schuster, R. Vazquez, and M. Krstic. Stabilization of linearized 2d magnetohydrodynamic channel flow by backstepping boundary control. *Syst. Control Lett.*, 57(10):805–812, 2008.

[40] H. Yu, R. Vazquez, and M. Krstic. Adaptive output feedback control of flow-induced vibrations of a membrane at high mach numbers. In *Proc. 56th IEEE Conf. Decis. Control*, pages 670–675, 2017.

[41] J. Zhang, R. Vazquez, J. Qi, and M. Krstic. Multi-agent deployment in 3-d via reaction-diffusion system with radially-varying reaction. *Automatica*, 161:111491, 2024.